

Implementation of Active Flow Control using Microjets on an RC Aircraft

A design package

Presented to

The Department of Mechanical Engineering

At Florida State University

In partial fulfillment

Of the requirements for

EML4550 – Senior Design Project I

At FAMU-FSU College of Engineering

By

Phillip Kreth

Daniel Drake

Matt Tubtim

Sam Nabulsi

December 4, 2007

Abstract

The following report details a design to implement active flow control on a scale model remotely operated airplane through the use of microjets. This design project is being sponsored by Eglin Air Force Base and being conducted by the Mechanical Engineering Department of Florida State University to create a test bed for flow separation research. The system will allow air flowing over the wings of the model airplane to remain attached at a higher angle of attack. The microjets consist of approximately 350, 0.4 mm holes located on the top of the wing surface, normal to the surface. These jets form a line that parallels the leading edge of the wing. Compressed air is emitted from the jets causing mixing in the boundary layer which delays flow separation. After conducting research in methods of supply, an 88 cubic inch compressed air cylinder was selected for the delivery system. This tank will be partially recessed into the fuselage of the plane in the area where the landing gear connects to the airframe. This tank will be shielded by an aluminum plate and wrapped in foam for crash protection. An adjustable pressure regulator set to 13.5 psig will feed air through flexible rubber supply lines to the microjets located in the wings. Pressure losses will reduce the pressure to 10 psig at the microjets. The system will allow 30 seconds of test time per flight. The exact placement of the microjets is currently being determined from wind tunnel tests using tuft visualization on a two foot section of the airplane wing. Devices for measuring the performance of the plane have been researched and are currently being finalized. One method that will be used is a camera mounted on the plane during flight to view tufts attached to the wing. The system is predicted to reduce the minimum flight speed by 7.2%. Other performance improvements are being investigated but have not been finalized. The estimated cost of the system is \$1,587.09 and the completion date is scheduled for April 3, 2008.

Table of Contents

List of Figures	4
I. Introduction	5
<i>Background</i>	5
<i>Project Scope</i>	6
II. Needs Assessment	7
III. Concept Generation, Analysis, and Selection	8
<i>Air Supply Method</i>	8
Pump/Compressor.....	9
Liquid CO ₂	9
Liquid N ₂	10
Compressed Air Cylinders	10
<i>Air Supply Method Selection</i>	10
<i>Data Measurement Devices</i>	12
Radar Gun	12
Crude Measurement Techniques.....	13
Obstacle Course	13
Streamers.....	14
Video Camera	15
GPS, Pitot Probe, Accelerometers	15
<i>Data Measurement Devices Selection</i>	16
IV. Detailed Design	18
<i>Air Supply System</i>	18
<i>Airframe Modification</i>	19
<i>Wing Support Bars</i>	21
V. Wind Tunnel Testing	23
VI. Testing Metrics	24
<i>Performance Metrics</i>	24
<i>Procedures for Demonstrating Metrics</i>	26
VII. Conclusions	27
X. References	30
Appendices	31
<i>A: Product Specifications</i>	32
<i>B: Calculation: Jet Duration at 10 psig</i>	33
<i>C: Calculation: Pressure Drop through the Supply System</i>	36
<i>D: Calculation: Determination of the Struts' Location</i>	45
<i>E: Calculation: Velocity Measurements with respect to Weight</i>	47
<i>F: Pro/ENGINEER Drawings and Assembly Views</i>	49
<i>G: Additional Weight Considerations</i>	57
<i>H: Budget</i>	58
<i>I: Planning and Scheduling</i>	59
<i>J: Gantt Chart</i>	61

List of Figures

<i>Figure #</i>	<i>Description</i>	<i>Page #</i>
1	Microjets	5
2	PDI screenshot of flow separation	6
3	Air supply conceptual drawing	8
4	Design Matrix – Air supply method	11
5	Radar gun illustration	12
6	Crude Measurement Techniques illustration	13
7	Streamer illustration	14
8	Video camera illustration	15
9	Design Matrix – Measurement Techniques	17
10	Diagram of the air supply system	18
11	Graph: Pressure loss vs diameter of the supply line	19
12	Placement of the tank	20
13	Diagram of the wing support system	22
14	Wind tunnel testing screenshot: Tuft test	23
15	Detailed diagram of the final system implemented	28

I. Introduction

Background

Research in active flow control systems has demonstrated the ability to control flow attachment and nose abatement in the laboratory. One of these systems, microjet arrays, has been successfully tested on a number of flow control situations. For this project, they will be used for flow reattachment. The microjets are 0.4 mm holes through which air is pumped out at pressures around 10 psig (Fig. 1).

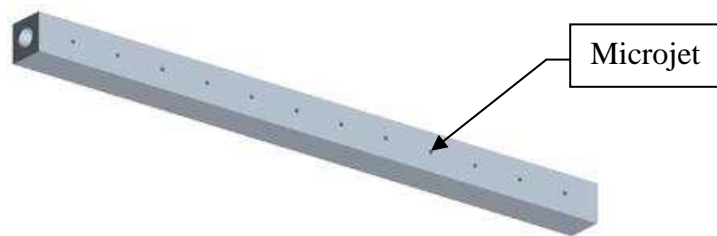


Figure 1: Microjets

The air is not used as thrust to propel the aircraft; instead, the pressurized air is forced out perpendicular to the airfoil's surface and the flow. This is used to cause mixing in the boundary layer in the region where flow separates from the wing during flight at the critical angle of attack (AOA) (Fig. 2). The placement of the microjets is crucial for the system to work efficiently. Research indicates that the jets should be placed just before the point of separation on the airfoil. The microjets once activated should allow the flow to remain attached at higher angles of attack. This means that the airfoil should still be producing lift at angles higher than the unmodified critical AOA.

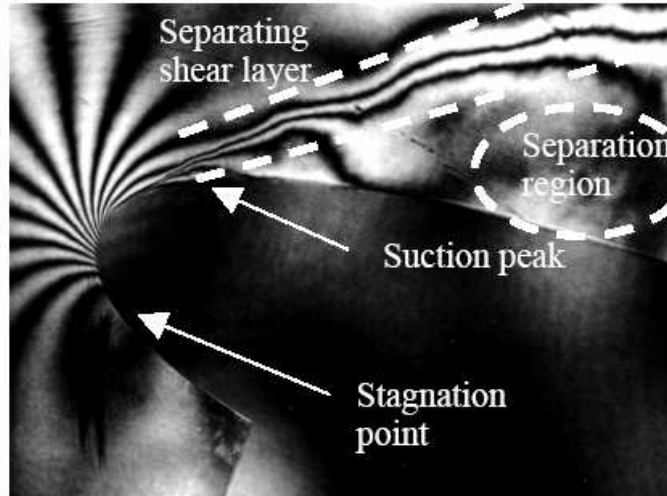


Figure 2: Flow separation on an airfoil beyond the critical angle of attack

Project Scope

The expectation of the project is to have an aircraft with microjet arrays on the wings that will increase the overall lift and delay stall. In order to do that, a model aircraft should be found and assembled. In considering the type of model, it is imperative that the aircraft be capable of holding the necessary hardware. After the assembly of the model is complete, the group should become familiar with the flying characteristics of the particular model. This can be done through flying practice without any hardware installed. Wind tunnel testing will be done on a wing section from the aircraft. These tests will determine the critical AOA and the separation point. Lift and drag measurements will also be made. Compiling the analyzed data, the group will implement the microjet arrays on the aircraft and acquire data to demonstrate the performance improvements.

II. Needs Assessment

1. Implement an active flow control (AFC) system, in this case microjet arrays, on a remote controlled (RC) aircraft
2. The system needs to operate for a long enough period of time to allow for testing and data collection
3. A budget of \$1500 should be maintained
4. The system should increase overall lift and delay stall
5. The microjets on the wing tips must be capable of individual activation to demonstrate roll control
6. The system needs to be activated remotely
7. An analysis of the flight characteristics that are going to be improved will be conducted

III. Concept Generation, Analysis, and Selection

For this project there are two major requirements. The first is the method in which to supply compressed air at 10 psig to 360 microjets. The second is measuring plane performance. Because of weight, volume, and budget constraints the systems will have to be selected in conjunction. The microjets themselves are simple and examples have been provided to us by our sponsor.

Air Supply Method

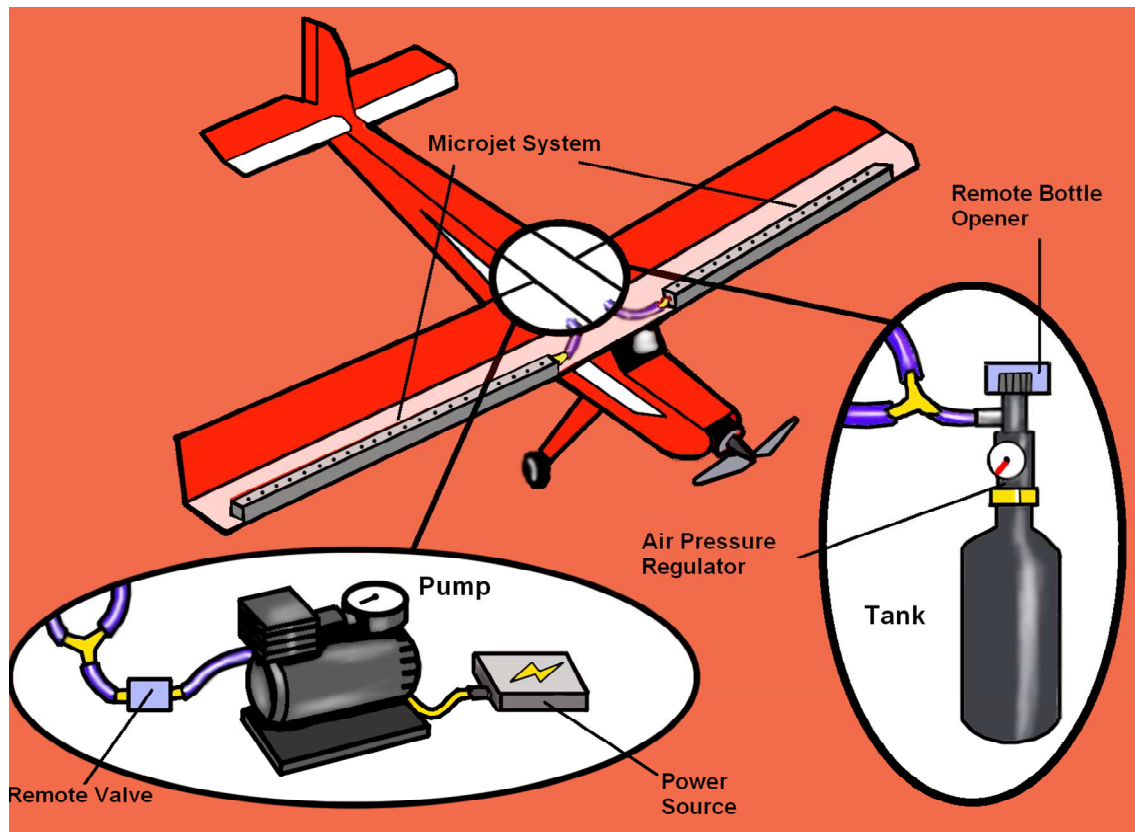


Figure 3: Two air supply concepts, one using an air pump the other relying on a tank.

The pump requires a power supply and a remotely operated valve. The tank filled with liquid CO₂, liquid nitrogen, or compressed air will require a remote valve and a pressure regulator. The selected systems will need to be housed in the cockpit area of the airplane.

Pump/Compressor

Several pumps were investigated to supply compressed air (Fig. 3). The weight of the system compared to the mass flow it can provide, and size, is a major factor and ruled out many pumps. The most suitable pump weighs 5.3lbs, consumes 75 watts at 12V, and can supply at least 20% more mass flow than required for 1 row of microjets. This pump cost \$320 dollars and has dimensions of 7.5in by 5in by 6.75in. A pump would also require an electrical power supply. This power could be supplied by batteries but would add as much as ½ lbs to the plane in order to supply power to the system for the duration of one flight. The major benefit of using a pump is its endurance. It can allow the system to run longer than any other proposed designs. Its major drawback is weight and cost.

Liquid CO₂

Liquid CO₂ is a common method for supplying compressed gas. It is found in systems to supply soft drinks, pneumatic tools, and fire arms. While they offer basic performance, they also are very affordable with a 22oz tanks starting at about \$20. Because the CO₂ is a liquid it is capable of supplying a large mass of gas for the volume it will occupy in the airplane. A 22oz tank would supply at least 50 seconds of system operation. This tank is 2.5 inches in diameter and 14 inches in length. CO₂ tanks are filled with liquid which turns to a gas after leaving the supply tank. The problem with this is that the temperature of the tank and supply lines drops as the fluid changes state. If enough CO₂ leaves the tank at a high enough rate, there is a possibility of the tank and line freezing. If enough heat is not added to the CO₂ it may remain liquid at the point of ejection and have undesirable effects on flow over the wing. Refills can be expensive when compared to refilling compressed air tanks. Another concern is the weight of the tank. These tanks are constructed of metal and tend to weigh more than some tanks used for compressed air applications. Also, the liquid inside the tank can move during flight which could cause problems with weight and balance in mid flight. This system would also require a pressure regulator. Still, liquid CO₂ tanks affordability make it a attractive choice.

Liquid N₂

Liquid nitrogen has some of the same benefits as the liquid CO₂. It is dense and is capable of supplying a large mass flow rate to the microjets. Containment is the major issue here. The liquid nitrogen cannot be placed into a closed container because of the high pressures that this would create, which may lead to an explosion. Designing a vented container that can operate at all flight attitudes adds complexity to the system. Also liquid N₂ has the same freezing problems as described above.

Compressed Air Cylinders

Compressed air cylinders are a common means of supplying air, for example SCUBA, cutting torches, and pneumatic tools. High pressure (HPA) tanks in particular are light weight, small, and affordable, these tanks are commonly used in tournament paintball games. A HPA tank with dimensions of 3.5 inches in diameter and 14 inches long is capable of supplying the necessary mass flow rate for 50 seconds. Also using compressed air does not lead to tank or line freezing. With only air inside the tank, the weight will not shift inside the plane which is important for weight and balanced. Another nice feature is that most HPA tanks include an integrated air regulator which can adjust outlet pressure. With less components to add the HPA tank is more space efficient. While HPA tanks have many good qualities they also have disadvantages. The compressed air may pose a hazard in the event of a crash and compared to liquid CO₂, HPA tanks cost more ranging from \$65 to almost \$300.

Air Pressure Regulator

Many of the tanks described above will need to use a regulator to bring the outlet pressure to 10 psi. Regulators come in two different styles, low and high pressure. For our purposes we need a low pressure regulator which would be able to regulate between 0 and 600 psi. Weight should not be much of an issue because many regulators are made of aluminum and are compact weighing less than ½ lb. Average cost of a regulator ranges from \$40 to \$60.

Air Supply Method Selection

The group utilized a design matrix (Fig. 4) to decide on the method to supply compressed air to the microjets. Upon inspection of the design matrix, one can see that the compressed air

tank has been selected as the optimum method. The design matrix has accounted for the weight and performance being the major factors in the selection process.

	Cat Wt	Weight	Pump	Liquid CO ₂	Comp. N ₂	Liquid N ₂
Safety	15					
For the Airplane		15	4	2	1	1
Cost	10					
Of Item and Use		10	3	4	3	3
Availability	10					
Of the Item		10	1	4	5	3
Performance Rating	25					
Of the supply method		25	0	2	5	2
Restrictions	40					
Weight		30	0	4	5	2
Volume		10	0	5	4	2
Total	100		1	3.3	4.1	2.05

Weighted Values for subcategories (these total up to the Cat Wt value).

These are the assigned scores for each option's category (0-5 possible points)

Resulting scores are shown at the bottom of each option

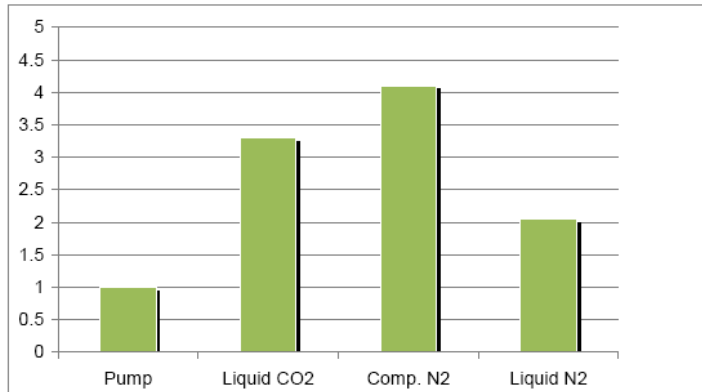


Figure 4: Design Matrix for the air supply method. The categories were selected and assigned a weighting factor as shown.

Data Measurement Devices

This section refers to the method of data acquisition once the entire system has been implemented to the aircraft. The group has chosen a couple of different options to try to obtain measurable values for certain flight parameters that will prove the concept.

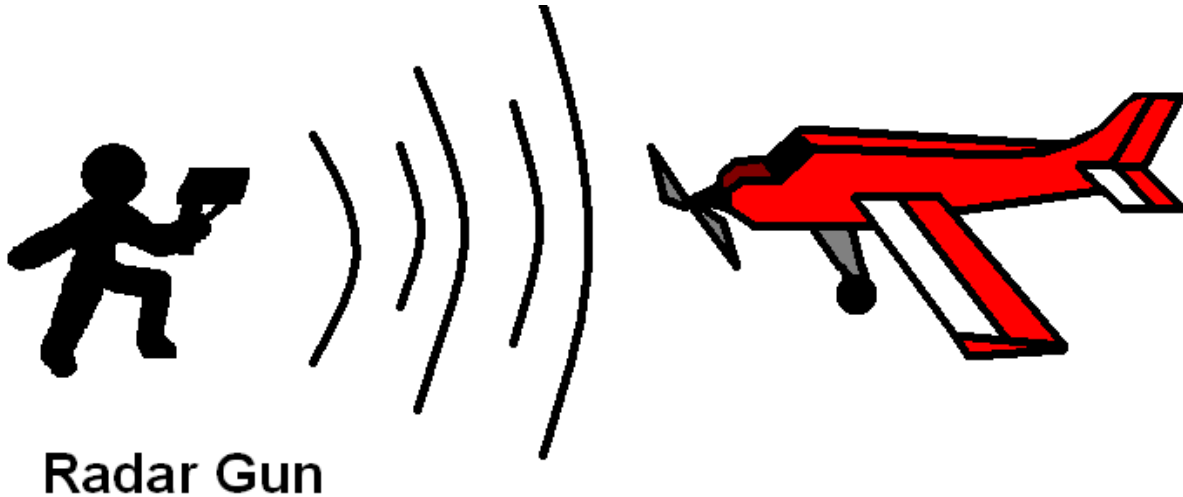


Figure 5: A radar gun can be used to measuring ground speed

Radar Gun – Sports Radar Gun from Bushnell - \$68.99 (Fig. 5)

- Easy to use: the gun has a rubber handle and the design allows for “point-and-shoot” measurements
- Large, clear LCD output
- Both mph and kph speeds can be reported
- Fastest speed is displayed when the trigger is released
- Accuracy is very high - +/- 1 mph and +/- 2 kph
- Safety depends on the measurements that are trying to be recorded:
 - If the climb rate is to be measured, a person might have to be on the runway directly under the airplane. This is a very risky situation and is also not allowed at the airfield.
 - The radar gun allows for measurements from 10 – 110 mph from 90 feet away
- The weight and volume of this device does not have an effect on the airplane’s performance or weight and balance.

- There is a major drawback to this measuring device when comparing it to the GPS device. The angle of incidence of the airplane velocity relative to the observer will change the speed displayed.

Crude Measurement Techniques

This covers a broad range of techniques that can be used to measure the airplanes performance. Some of the design ideas include setting up an obstacle course next to the runway and taking video measurements. Another design concept is putting streamers on the airplane to determine the angle of attack.

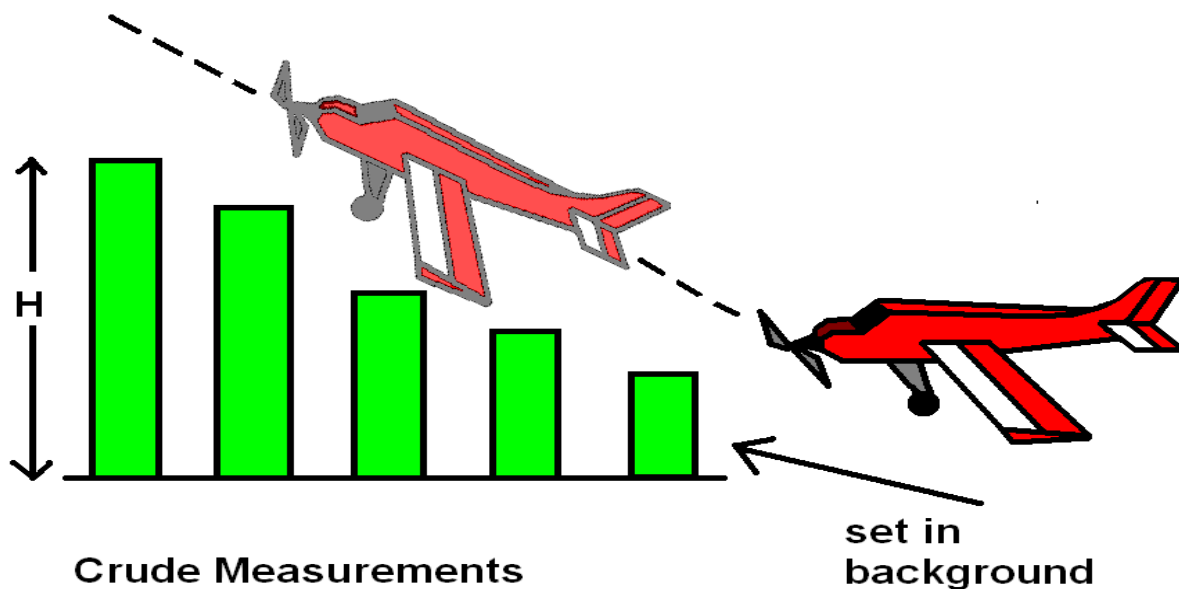


Figure 6: Measuring angle of climb using pylons placed in the background and video recording the flight with a camera mounted on a tripod. Climb angles can be compared with the system on and off

Obstacle Course (Fig. 6)

- The supplies used to build an obstacle course could probably be borrowed or made out of scrap. The price for the obstacle course is estimated to be very low.
- The setup of the obstacle course is pending, but some ideas are as follows:
 - Beams of varying heights may be set up parallel to the runway and when the aircraft takes off, the distance to the objects may be measured. The airplane should climb over the obstacles in a measured time and the rate of climb calculated.

- Slow flight speeds could be measured by setting up the same beams parallel to the runway and inspecting video evidence of the airplane flying behind the beams if they are placed at certain distances apart.
- This may be a risky measurement technique. The airplane, should it lose control, may crash into some of the obstacles and suffer damage.

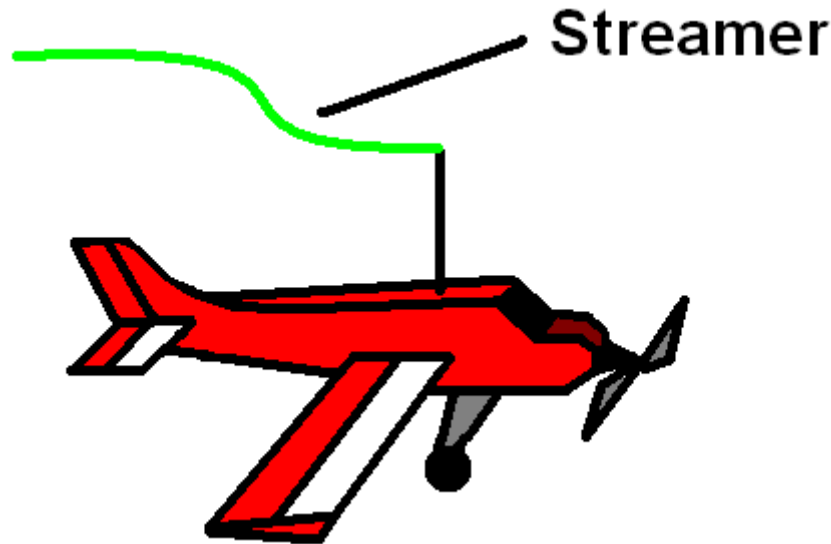


Figure 7: Using a streamer that is mounted outside of the plane's wake the angle of attack can be determined by capturing images of the plane in flight and comparing the streamer and wing angles. This technique is limited to non accelerated flight

Streamers (Fig. 7)

- Streamers are cheap to buy and relatively easy to implement on the aircraft.
- An overhead design will allow for these to stay out of the way of the airplane and allow for unmodified takeoff and landing. This should also keep the streamers out of the wake regions behind the aircraft and its wings.
- The streamers, coupled with video evidence, will give the team the angle of attack.
- The drawback is the uncertainty in measurements may not be known.



Figure 8: Video recording the flight is a simple and inexpensive means of measuring plane performance. The video will have to be shot in a consistent location and angle for accurate comparisons to be made.

Video Camera (Fig. 8)

- A tripod can be used to maintain a stable point-of-view.
- This will actually limit the range that the video camera can capture.
- The cost of this is virtually zero since the camera can be borrowed and data can be exported to a computer.
- The camera will not affect the weight and balance of the airplane since it does not need to be implemented.
- This is a very safe method of capturing data since nothing has to be mounted on the airplane and no group member has to be near the flying area.
- The major drawback about this measurement device is the accuracy. While some of the video may look very presentable, the accuracy of the data acquired from the video may not be known.

GPS, Pitot Probe, Accelerometers

One option for measuring plane performance is a GPS system that is already commercially available for measuring the performance of model airplanes. This device mounts inside the airplane and can record data, or wirelessly send the data real time to a computer. This system can measure airspeed using a pitot probe, measure groundspeed, altitude, and rate of climb using GPS, and measure acceleration using an accelerometer. This system is also capable

of measuring plane attitude using gyros but this add-on is considerably more expensive. This complete system weighs less than a ¼ of a pound. The resolution for airspeed and altitude is 1mph and 1ft respectively. The angle resolution for the gyros is 1200 degree-seconds. The cost of the base unit which measures climb rate, airspeed, and groundspeed is \$449.99, the accelerometer for G measurements is \$79.99, the cost for the gyros is \$1,449.00. The volume of the complete system is less than 10 in². Although the resolution of the GPS is good its accuracy may be poor. The sponsor of the project has used GPS on model aircraft and has found that the accuracy necessary for rate of climb measurements for this project is not possible using GPS.

Data Measurement Devices Selection

The group has decided to utilize a design matrix (Fig. 9) to select a design from the list of possible data measurement techniques. Again, weight and performance are the main factors in the selection process. While the design matrix suggests that the GPS system be used, after meeting with the sponsor, the group has decided against using GPS. During the meeting at Eglin Air Force Base, measurement techniques were discussed and the accuracy of the global positioning systems used in RC aircraft was brought up. It was concluded that a GPS that would fit within our budget constraints would not produce accurate results. Instead, a servo-mounted camera setup was suggested. This would allow for the user to watch the effect of the microjets on tufts placed on the wings. These would easily show, on a video monitor, that stall is occurring and that the flow is being reattached with the microjets on.

	Cat Wt	Weight	Radar Gun		Camera		GPS		Crude Measurements	
Safety	15									
For the Observer		15	2	30	4	60	5	75	2	30
Cost	10									
Of Item and Use		10	4	40	5	50	1	10	5	50
Availability	10									
Of the Item		10	4	40	5	50	5	50	4	40
Performance Rating	25									
Of the measurements		25	1	25	0	0	5	125	0	0
Restrictions	40									
Weight		30	5	150	5	150	4	120	3	90
Volume		10	5	50	5	50	4	40	3	30
Total		100		3.35		3.6		4.2		2.4

Weighted Values for subcategories (these total up to the Cat Wt value)

These are the assigned scores for each option's category (0-5 possible points)

Resulting scores are shown at the bottom of each option

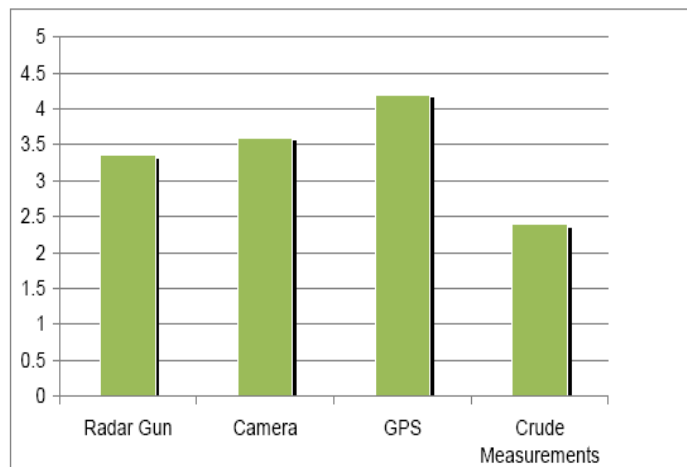


Figure 9: Original Design Matrix for the measurement techniques. As can be seen GPS had the highest rating but was removed with the advice from the project sponsor. Camera techniques was then selected and other methods are still being considered.

IV. Detailed Design

Air Supply System

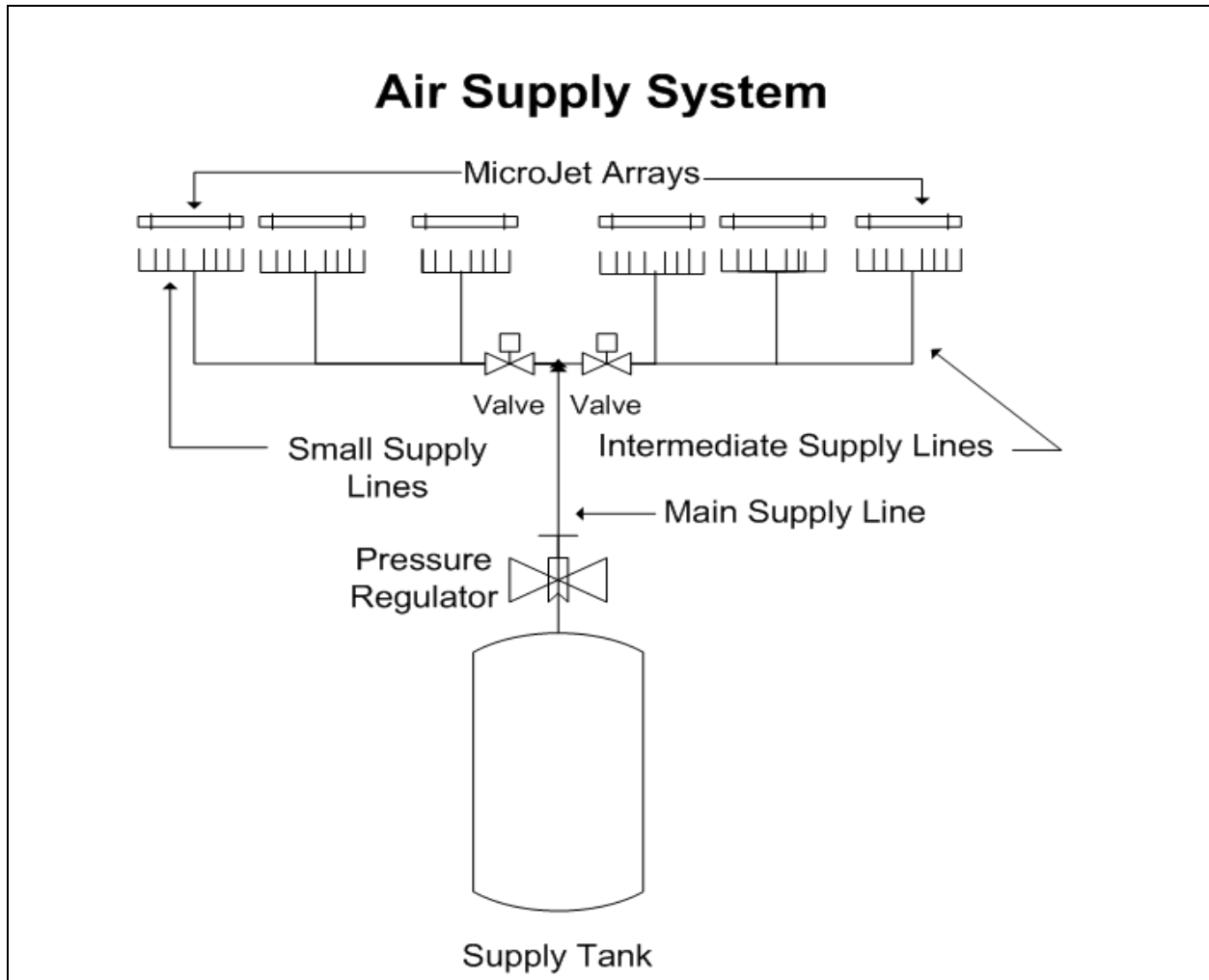


Figure 10: Diagram of air supply system. Air travels from main supply line to the intermediate supply lines then to the small supply lines which feed the microjets. A pressure regulator is located between the tank and main supply line. Two electric valves are located in the intermediate supply lines.

The pressure losses for each of the three supply lines utilized in the design was calculated and graphed as a function of their diameter; calculations are located in Appendix C. From the graphs it was clear that the pressure losses rise asymptotically when the supply line diameter is reduced to a critical size (Fig. 10). From these graphs supply line diameters were selected to keep the total loss in the supply system below 7.4 psia so that incompressible flow analysis

would be valid. The other selection criterion was to minimize the diameter of the supply lines in order to minimize weight.

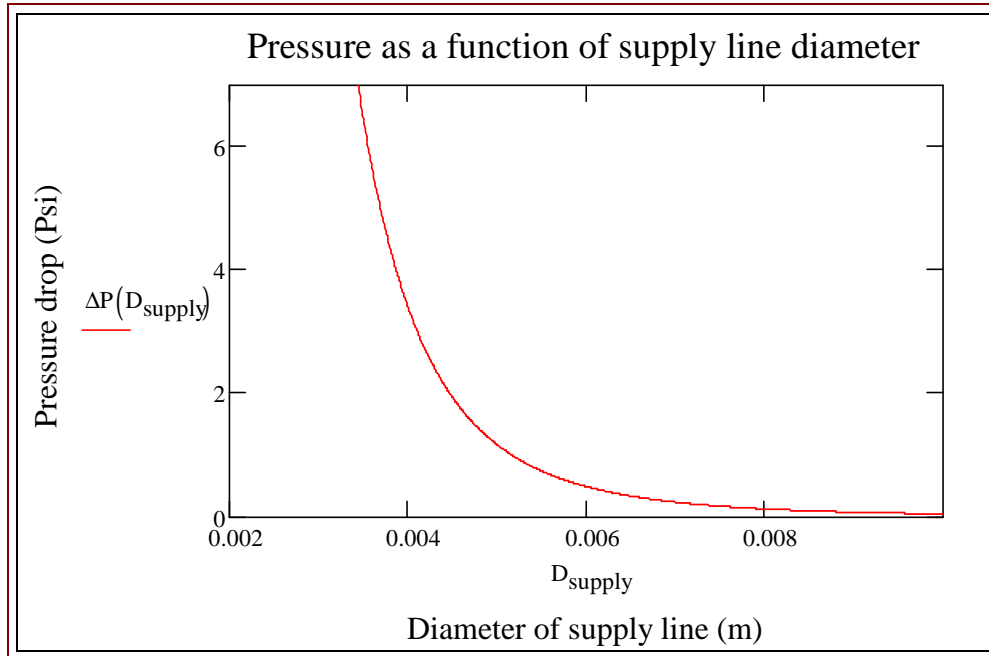


Figure 11: Pressure loss as a function of the diameter of the intermediate supply line. From the graph it is apparent that the pressure drop rises asymptotically near 4mm. From this a supply line diameter of 6mm was chosen with a pressure drop of 0.489 psi over a four foot section.

Pressure losses in the distribution manifold, valves, and at the microjets were also calculated and added to the losses in the supply lines (Fig. 11). The total loss for the air supply system was 3.53 psi. This is well within the 7.4 psi limit for incompressible flow analysis for this system. The assumption that the density is constant will only lead to errors on the order of 10%². The total weight of the tubing was also calculated and is 0.53 lbs. Also to keep the pressure drop from the tank to the microjets the supply line will all be the same length. For example all the small supply line will be 8in long and all the intermediate supply lines will be 4 ft long. Pressure ports have been incorporated into the microjet arrays in order to test the pressure of each array.

Airframe Modification

In order to activate the microjets, air must be supplied by some outside source. The most suitable method found was using a high pressure air tank. Since the tank will be over three

inches in diameter, fully enclosing it within in the plane is not an option. While placing the tank on the top center of the wings would be safest during a crash, aerodynamics will be affected. The best option was to mount the tank to the bottom of the plane. This method posed two problems. With the tank being mounted so low, a clearance issue with the landing gear became apparent. Also with the tank being exposed on the bottom, the chance of puncture during a crash could cause an explosion. Therefore, the main concerns became safety and practical integration with the plane. The main way to address this problem was to create a shield that could protect the tank and also incorporate it as a part of the airframe.

The goal of the tank location is to make sure it is integrated with the plane but still could be accessed for maintenance and ease of refilling. First, the location of the tank was marked on the plane taking into the account the balance of the aircraft. From the markings, the plane's structural pieces would be cut from the bottom allowing for some of the tank to be recessed within the plane. This would make the assembly more compact, able to clear the landing gear, and provide some top shielding to the tank (Fig. 12). With the bottom now exposed, shielding must be made to protect the tank from a crash.

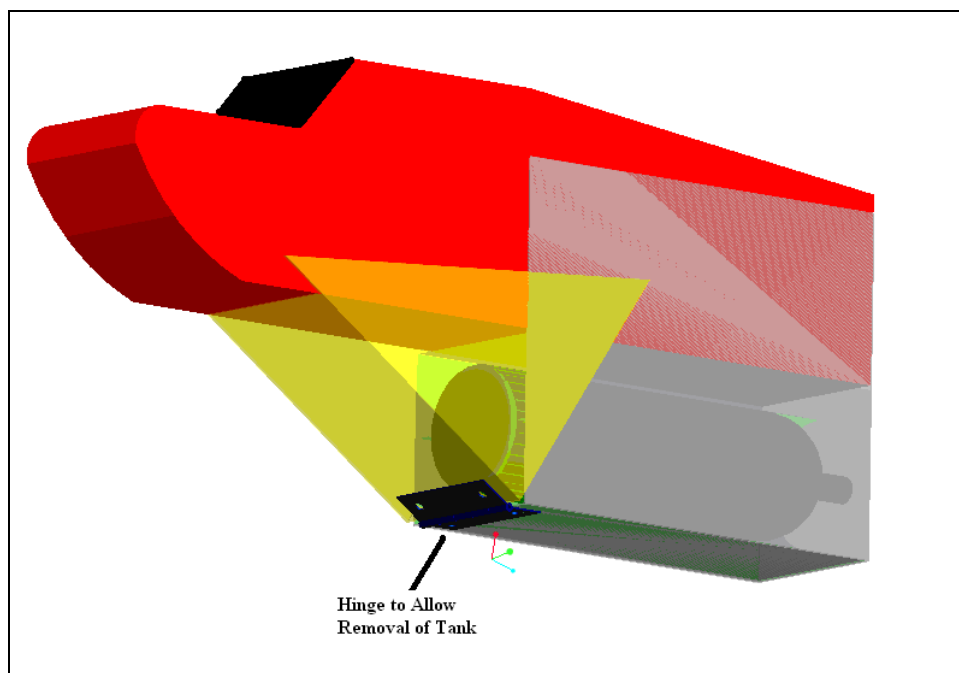


Figure 12: Placement of the compressed air tank.

The shield works by splitting it into two parts. The first part encases the tank with molded foam supports which will displace energy around the outside of the tank during impact.

The sides of the shield will bolt to the sides of the plane. Not only will the shield fully enclose the tank, but it will add structural rigidity to the plane. The material for the shield will be aluminum sheet metal which should be sufficient to protect the tank and keep weight down. The second part of the shield is the nose. It will bolt partly to the plane and partly to the first shield. The nose closes off the front of the shroud reducing drag. Using a hinge assembly the nose can be lowered for easy removal for tank refilling. The space in the nose can also house more protective foam and air supply line tubing. In the event of a frontal crash the nose's angled design can protect the tank from taking head on collision.

The dimensions of the shield take into account the size of the tank and foam core which are shown in the drawings. With the shield, the tank should be protected and the plane body will be strengthened. Another advantage of having the shield is its function as an extension of the plane's body which will provide lower mounting points for the struts. As explained in the design of the struts, the lower mounting points will offer reduced loads to the planes wings. All engineering drawings are located in Appendix F.

Wing Support Bars

This design project will require adding some weight to the remote controlled aircraft. In RC aircraft, as in real flight, the weight and balance of the aircraft is very important. While the airplane used in this project will be able to support the added weight, it is necessary to support some of the weaker locations of the airframe. The weakest connection of the airframe is located at the wing's connection to the fuselage. The kit for the aircraft has simple rubber bands used to hold the wings in place. These are not rigid and have failed during flights with increased weight. Struts will be used to increase the rigidity and strength of the connection of the wings to the fuselage. We have calculated that the placement of the struts will be at a location of 16.4" down the wing from the fuselage and 11.5" down the fuselage from the bottom surface of the wing. The second location is lower than the actual surface of the fuselage extends, but placement here is possible since we are extending the fuselage lower with the placement of the compressed air tank.

We have determined from a force and moment balance that this location is going to be the optimal location for our airframe. The distance along the wing's surface has been determined to be at the location of the center of the wing. This will keep the force in the normal direction at

an average value: equal to the lift force produced by each wing. As one will see in Appendix D, moving this location closer to the fuselage will increase to force in the normal direction. This is the exact result that we do not need. Conversely, moving the location further from the fuselage will lower the force in the normal direction. While the optimum placement for this location would be at the wing tip, this is not feasible. We have determined to place the mounting bracket on the location nearest the center of the wing. If this location is already taken (by the servo or a support spine), we will move it to the next possible location further from the fuselage.

The height of the struts has been determined by looking at the force that would compress the wings. This force must be as low as possible. By changing the location of the fuselage's mounting bracket to a lower position, the force is lowered. Optimally, this position would be as low to the ground as possible, but we must consider the clearance of the aircraft. We have also determined that the compressed air tank will be placed outside of the airframe and located below the fuselage. This will give us a lower location to mount the strut to on the fuselage, lowering the compressive force and maintaining a good clearance. This location is 11.5" from the bottom surface of the wing (Fig 13).

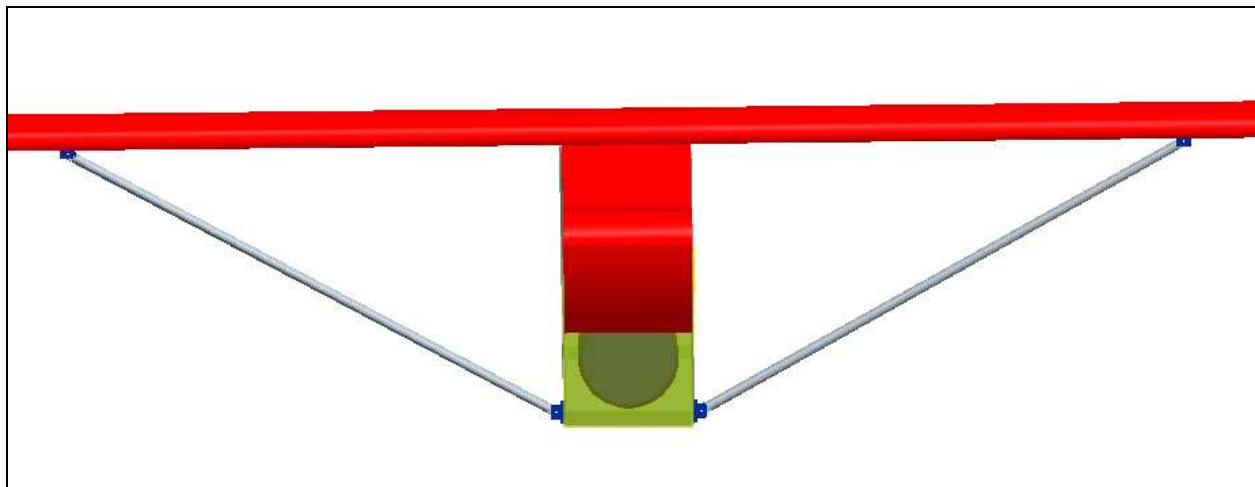


Figure 13: Frontal view of the wing support system. Shown in blue, the brackets will mount to the bottom surface of the wing and at the lower edge of the shield. Note that the entire wingspan has not been shown to allow a more detailed view of the system in this figure.

Engineering drawings for the supporting rod and bracket mounts have been attached in Appendix F as well.

V. Wind Tunnel Testing

Several wind tunnel testing techniques were used and are described below. The testing is not yet concluded but some of the preliminary results are available. Successful Tuft visualization tests were performed (Fig. 14), and a video of the test was taken and can be viewed at http://www.eng.fsu.edu/~krethph/senior_design/tufttest.wmv. This test used small wool yarn taped to the surface of the wing. The test section was then run at 10m/s and the angle of attack varied from 0 to 20 degrees. Separation occurred at approximately a 16 degree angle of attack. The test also shows a rough location of separation. This test will be particularly useful for demonstrating flow reattachments with the microjets implemented and activated.



Figure 14: Tuft visualization test. From the image separation is evident from the tufts bending as the flow reverses direction. This is more apparent towards the centerline of the wing where the wind tunnel walls have no effect on the flow.

Paint tests were also conducted. This test utilizes an oil and dye mixture that was applied to the wing surface in small droplets, the liquid resembles white paint hence the name. Although the test shows movement of the droplet the images taken were questionable when viewed by an expert. The test main fault was a lack of video record. The images captured were still images. The current results are inconclusive and future testing will resolve this issue.

VI. Testing Metrics

Performance Metrics

To demonstrate the increased performance from the use of the active flow control system the following flight parameters will be tested with the microjet system activated and compared to the flight characteristics without the jets. Operating the jets should actively attach the flow and increase the critical angle of attack of the aircraft. This will produce greater lift and drag than the unmodified airplane. The following flight maneuvers will be tested.

- 1) *Takeoff Distance and Touch Down Speed* - The plane should have reduced takeoff roll with jets activated. During short field takeoff, with the wings near the critical angle of attack during roll, the plane will produce sufficient lift to take off at lower airspeeds (Eqn. 1.1). From the research of Michael Amitay, Flight Control Using Synthetic Jets³, it was shown that an increase in lift of 16% is possible. Using that as the basis for velocity calculations and reference values for the coefficient of lift from Theory of Wing Sections⁴, a 7.2% reduction of landing speed can be shown. For an aircraft weight of 8 pounds this would be a reduction of 1.3 miles/hour.

$$\text{Lift} = \frac{1}{2} \cdot V^2 \cdot A \cdot C_L \quad (1.1)$$

V = Airspeed

A = Wing Area

C_L = Coefficient of Lift

As can be seen from equation 1.1, increasing the critical angle of attack increases the coefficient of lift. The lift value for takeoff corresponds to the airplane weight for non accelerating flight. This is valid at the point of takeoff. With the lift value fixed and the coefficient of lift increasing, the airspeed (V) decreases. However the drag is also increased with increasing angle of attack, typically at an exponential rate. It is necessary that the plane produce sufficient thrust to overcome the additional drag force. Using a large coefficient of lift the power necessary to overcome drag was calculated to be 11% of the available engine power. For the case of touchdown speed engine power is not an issue. In this situation the drag force works to reduce the kinetic energy of the landing plane. As the landing plane

dissipates its kinetic energy it will pass through the point where the lifting force is less than the weight of the aircraft and the plane will touchdown in a stalled condition. This maneuver is common for landing planes. The touchdown speed will be reduced as the angle of attack is increased as described above. For both cases the required runway length will be reduced demonstrating a useful increase in performance. Also for a landing aircraft the microjet system can be powered with the surplus engine power that a landing plane has at partial throttle, with no adverse effect on thrust.

- 2) *Minimum Controllable Airspeed* - Positive roll control can be maintained at a lower airspeed with wing tip microjets activated delaying stall over the portion of the wing with ailerons. This can be demonstrated by measuring airspeed while simultaneously videoing tufts mounted on the wings. The wing roots should show flow separation while the flow over the wing tips remains attached. The velocity of the plane relative to the incoming air for this test is 7.8m/s which is the same velocity for test 1.
- 3) *Maximum Angle of Climb* - During climb the plane can maintain a steeper angle of attack with the microjets on which will increase drag and cause reduced air speed for a given thrust (power setting). If the reduced lift as a result of lower airspeed is offset by the increase in lift from a higher angle of attack the plane will have a greater angle of climb. This will result in improved obstacle clearing (Trees/power line at the end of the runway).
- 4) *Roll Control Using Wing Tip Jets Only* - Activating the microjets on one wing should create asymmetric lift and cause the plane to bank. This is more likely to occur at AOA greater than 5 deg. At these angles the mixing caused by the microjets will increase the flow velocity over the trailing edge of the wing resulting in higher lift. This flow modification is not as effective at low angles of attack. For this control technique to work the increased lift will have to be larger than the thrust produced by the microjets.
- 5) *Rate of Climb*- Rate of climb may also be improved due to improved flow over the wing but has not been quantified yet.

Procedures for Demonstrating Metrics

The following test should be conducted during periods of steady atmospheric conditions, for example wind speed, wind direction, atmospheric temperature and pressure. The plane should have consistent weight, balance, and power output.

- 1) Take off distance will be measure by video recording the takeoff. The plane will start rolling at full power at a consistent starting point on the runway. The tail wheel of the plane should remain in contact with the runway until takeoff to maintain a constant angle of attack. Using preplaced markers the takeoff distance will be determined by replaying the video and observing the takeoff point. Several test runs should be performed with the microjets activated and off to judge the most appropriate placement of the runway markers. Also, the correct timing for activating the microjets should be estimated, ideally the microjets would activate at a ground speed sufficient for liftoff. The runway markers should be spaced evenly and their placement recorded. This test should be repeated at several different angles of attack to determine minimum runway takeoff distance. Touch down speed can be measure with a radar gun or by use of a pitot probe. For this test the plane should land in a stalled condition.
- 2) To demonstrate control at lower airspeeds with the jet activated the plane should first climb to an altitude to allow for recovery from a stall. Then the plane should be flown in level flight with the jets on. The plane should enter a stall while demonstrating roll control by rolling the plane back and forth. Airspeed should be recorded along with video of the tufts mounted on the wing.
- 3) Maximum angle of climb procedures have not been finalized.
- 4) Roll control using the microjet will be demonstrated by activating jets on individual wing during level flight. The plane will be flown thru 180 deg turn using only the jets for roll.
- 5) Rate of climb procedures have not been finalized.

VII. Conclusions

The final selection and design of a system to supply air to an array of microjets has been detailed in the preceding report. This system will use a compressed air cylinder and pressure regulator to supply at least 30 seconds of air to the required 6 feet of microjets. The supply line will have a 3.5 psi drop in pressure from the tank to the microjet arrays. The length and diameter of the tubing have been calculated. The tanks location and mounting have been determined along with a system to protect the tank in the event of a crash. A design to modify the plane to hold the additional 6.08 lbs of weight has also been detailed. These modifications include adding struts and securely attaching the wings to the fuselage. The necessary component for the supply system have been identified and priced and suppliers have been selected. The specific locations of the microjet arrays are currently being determined using Tuft visualization technique in a wind tunnel. Some testing metrics are defined such as the 7.2% reduction in minimum airspeed and takeoff distance. However, rate of climb has yet to be quantified. The total cost of implementing the design is projected to be \$1,381.93 which includes 20% for price overruns. With the exception of wind tunnel testing and finalization of the measuring devices all tasks on the original schedule have been completed. A diagram of all modifications to the airframe can be seen on the next page (Fig. 15).

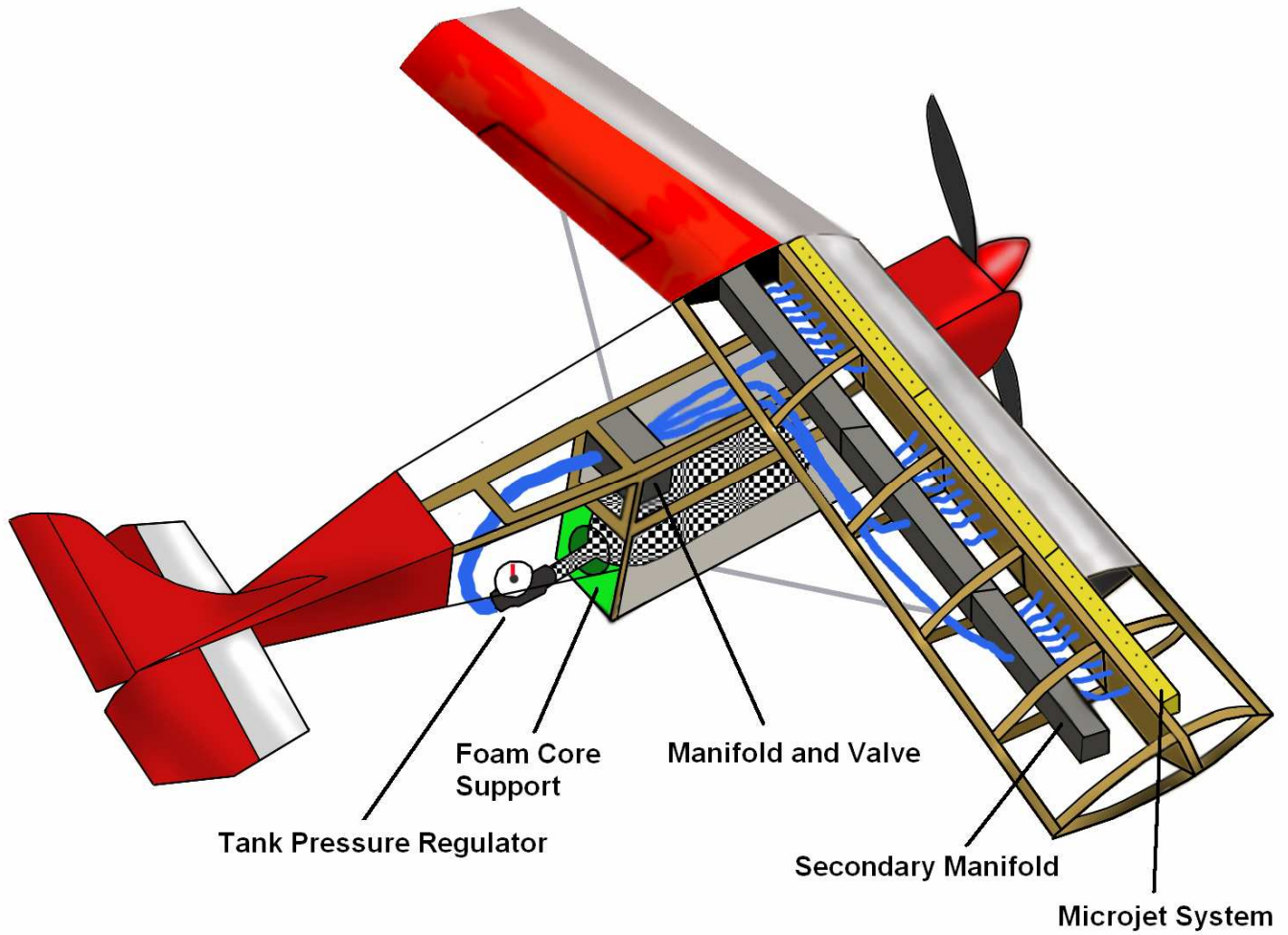


Figure 15: This diagram shows the entire system as it will fit on the airframe. The air supply system, wing support bars, and modified airframe are shown.

IX. Acknowledgements

We would like to thank several people for their assistance throughout the design phase of this project. Dr. Farrukh Alvi, Advanced Aero Propulsion Lab, is our faculty advisor and has provided valuable feedback on all of our work and given us an in-depth view on this project and its correlations to larger scale applications. Dr. Gregg Abate, Eglin Air Force Base, is the corporate sponsor for the project. He helped steer us in the right direction during our on-site visit to Eglin Air Force Base. Dr. Cesar Luongo is the professor in charge of the Senior Design I class. He has been a motivation to us as well as a supplier of extremely valuable input. He is always available to answer all questions we can throw at him.

X. References

1. Shih, C., and J. Beahn. Control of Compressible Dynamic Stall Using Microjets. Joint Fluids Engineering Conference, 6 July 2003, Honolulu, HI.
2. Cengel, Yunus A., and Robert H. Turner. Fundamentals of Thermal Fluid Sciences. Boston: McGraw-Hill, 2005.
3. M. Amitay and A. Glezer, “Separation Control using synthetic Jet actuators”. Chapter in a book on Manipulation and Control of Jets in Crossflow. Series: CISM International Centre for Mechanical Sciences , Number 439. Editors: Ann R. Karagozian, Luca Cortelezzi and Alfredo Soldati, 2003, ISBN: 3-211-00753-9.
4. Abbott, Ira H., and A. E. Von Doenhoff. Theory of Wing Sections. Dover Publications, 1959.

Appendices

Appendix A

Specifications

General Description:

The product will use microjets installed on the wing of a remote controlled scale aircraft to actively control flow separation over the wings. The system must supply air or a gas with similar properties to the microjet array. The product should allow for performance measurements.

Design Constraints:

1. Total weight of supply system and jets - 6 lbs or less
2. Microjet run time - 30 seconds or greater
3. Gauge pressure at the microjets - 10 psi+
4. Microjet size – 0.4mm
5. Microjet spacing – 5mm
6. Number of rows of microjets along wing – 2 or less
7. Mass flow to the microjets - $4.4(10)^{-5}$ kg/s
8. Microjets activation- remotely, wireless for each wing individually
9. Volume of system – 6in × 6in × 15in or less
10. Minimum payload capacity for performance measuring equipment – 2 lbs

Aircraft Operating Parameters:

1. The airplane shall be able to land and takeoff unassisted, as it would in an unmodified state, with the exception of takeoff distance.
2. The plane shall be capable of recovering from a spin.
3. The plane's endurance will be at least 10 minutes.

In the event of a crash the systems on the aircraft will not pose a danger to the operator or spectators standing a distance of 100ft from the impact.

Appendix B

The following MathCAD document displays the microjet runtime as a function of the length of the array. The mass flow rate has been calculated and the graphs are displayed on the subsequent pages.

Calculating Jet Duration at 10 psig

$$\text{kJ} := 1000\text{J}$$

Gas Constants $R := .2870 \frac{\text{kJ}}{\text{kg} \cdot \text{K}}$

Temperature $T := (25 + 273)\text{K}$

Volume of Tank $V := 68\text{in}^3$

Tank Pressure $P := 4500\text{psi}$

Mass of air in tank $m_{\text{tank}} := \frac{P \cdot V}{R \cdot T}$ $m_{\text{tank}} = 0.404 \text{ kg}$

Pressure to the Jet $P_t := 1\text{atm} + 10\text{psi}$

Constant for Air $\gamma := 1.4$

Mass Flow Rate Per Micro jet assuming the jet is choked $P_b := \frac{P_t}{\left(1 + \frac{\gamma - 1}{2}\right)^{\frac{\gamma}{\gamma - 1}}}$ $P_b = 8.995 \times 10^4 \text{ Pa}$
 $\frac{P_b}{P_t} = 0.528$

Velocity of Jet exit $M_1 := \sqrt{\gamma \cdot R \cdot 273\text{K}}$ $M_1 = 331.197 \frac{\text{m}}{\text{s}}$

Radius of jet $r := \frac{.4\text{mm}}{2}$

Cross Sectional area of jet $A_{\text{cross}} := \pi \cdot r^2$

Calculated Mass Flow Rate per jet @ 24.7 psia $m_{\text{dot_calculated}} := \frac{P_b \cdot M_1 \cdot A_{\text{cross}}}{R \cdot T}$

$m_{\text{dot_calculated}} = 4.377 \times 10^{-5} \frac{\text{kg}}{\text{s}}$

Mass Flow Rate Per Micro jet from $m_{\dot{dot}} := \frac{.03 \text{ kg}}{500 \text{ s}}$
 Dr. Shih Research
 www.eng.fsu.edu/departments/
 mechanical/labs/hilites/presentations/
 fml/dynstall.pdf

$$m_{\dot{dot}} = 6 \times 10^{-5} \frac{\text{kg}}{\text{s}} @ 22 \text{ psia}$$

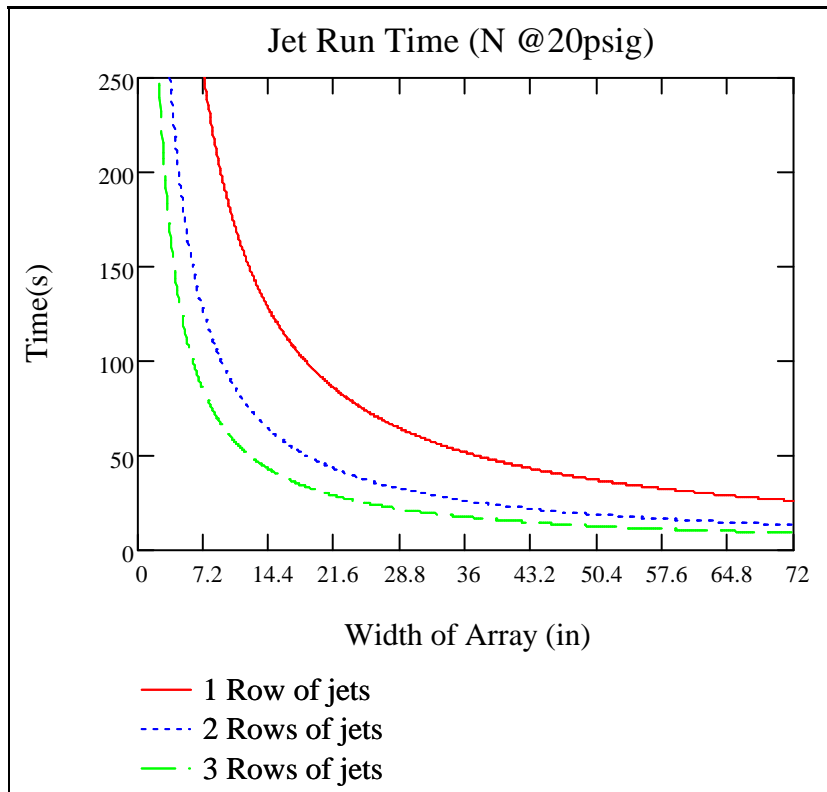
.4mm jet

Jet Run Time as a function of the number of jets

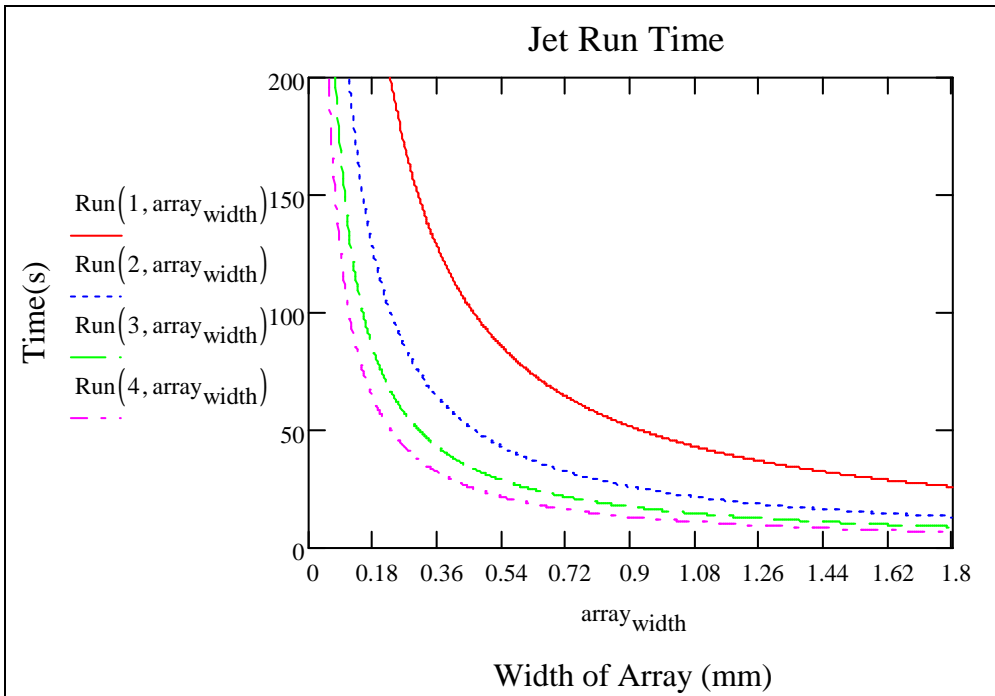
$$\text{Run}(\text{rows_of_jets}, \text{array_width}) := \frac{m_{\text{tank}}}{m_{\dot{dot_calculated}} \cdot \text{rows_of_jets} \cdot \text{array_width} \cdot \text{spacing}} \cdot \frac{1}{.025}$$

jet = 1

Jets per width of wing $\text{spacing} = \frac{1 \text{ jet}}{5 \text{ mm}}$



$$\text{Run}(\text{rows_of_jets}, \text{array_width}) := \frac{m_{\text{tank}}}{m_{\dot{dot_calculated}} \cdot \text{rows_of_jets} \cdot \text{array_width} \cdot \text{spacing}}$$



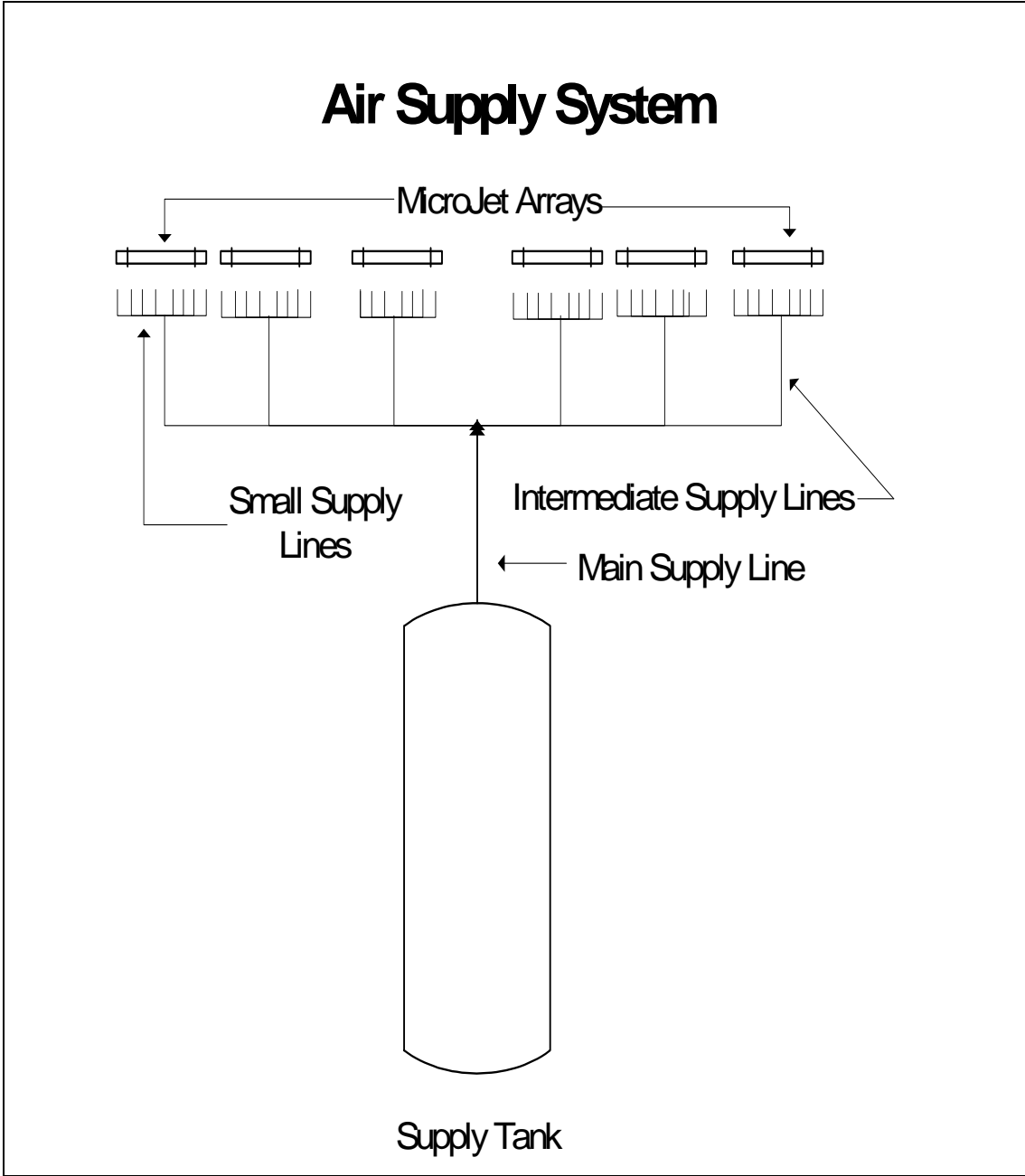
Volumetric flow through pressure regulator.

$$\frac{\dot{m}_{\text{calculated}} \cdot 365}{\frac{P_t}{R \cdot T}} = 17.004 \frac{\text{ft}^3}{\text{min}}$$

Appendix C

This appendix contains all of the calculations to determine the detailed design of the air supply system. The number of supply lines, microjets, and length of the supply lines are some examples of what was calculated.

Design Calculations for Air Supply System



Pressure Drop Calculation

Given Values

Color Code for worksheet	Design Variable	Results
Temperature of air from supply Tank	$T_1 := 298\text{K}$	
Gas Constant (air)	$R := \frac{287}{\text{kg}\cdot\text{K}}$	
Dynamic Viscosity of Air, (small error up to 7atms)	$\mu_{\text{air}} := 1.849 \times 10^{-5} \frac{\text{kg}}{\text{m}\cdot\text{s}}$	
Jet pressure	$P_{\text{jet}} := 10\text{psi} + 10\text{kPa}$	$P_{\text{jet}} = 24.649\text{psi}$
Jet Spacing	$\text{jet}_{\text{spacing}} := \frac{1 \cdot \text{jet}}{5\text{mm}}$	$\text{jet}_{\text{spacing}} = 0.2 \frac{\text{jet}}{\text{mm}}$
Wing length (actual wing length will be 5'9")	$L_{\text{wing}} := 6\text{ft}$	
Total number of jets	$N_{\text{jet}} := L_{\text{wing}} \cdot \text{jet}_{\text{spacing}}$	$N_{\text{jet}} = 365.76$
Number of Jet arrays	$N_{\text{array}} := \frac{L_{\text{wing}}}{1\text{ft}}$	$N_{\text{array}} = 6$
Density of Air at 10 psig	$\rho_{\text{air}} := \frac{P_{\text{jet}}}{R \cdot T_1}$	$\rho_{\text{air}} = 1.987 \frac{\text{kg}}{\text{m}^3}$
Mass Flow per Jet at 10psig	$M_{\text{jet}} := 4.377 \times 10^{-5} \frac{\text{kg}}{\text{s}}$	
Total Mass flow from tank	$M_{\text{total}} := M_{\text{jet}} \cdot N_{\text{jet}}$	$M_{\text{total}} = 0.016 \frac{\text{kg}}{\text{s}}$
Mass flow per array	$M_{\text{array}} := \frac{M_{\text{total}}}{N_{\text{array}}}$	$M_{\text{array}} = 2.668 \times 10^{-3} \frac{\text{kg}}{\text{s}}$
Maximum pressure drop to allow for incompressible flow analysis.	$P_{\text{jet}} \cdot 30\% = 7.395\text{psi}$	
Approximate length of intermediate the supply	$L_{\text{supply}} := 4\text{ft}$	
Approximate length of small supply lines	$L_{\text{small}} := 8\text{in}$	
Diameter of small supply line	$D_{\text{small}} := 1.6\text{mm}$	
Length of main line	$L_{\text{main}} := 1\text{ft}$	

Determining the diameter of the Intermediate supply line

Laminar Flow Analysis

The pressure drop across the large supply line is as followed

$$\Delta P = f \cdot \frac{L_{\text{supply}} \rho_{\text{air}} \cdot V_{\text{supply}}^2}{2D_{\text{supply}}}$$

Where

$$f = \frac{64}{\text{Re}} \quad \text{Assuming laminar flow.} \quad \text{Re} = \frac{\rho_{\text{air}} \cdot V_{\text{supply}} \cdot D_{\text{supply}}}{\mu_{\text{air}}}$$

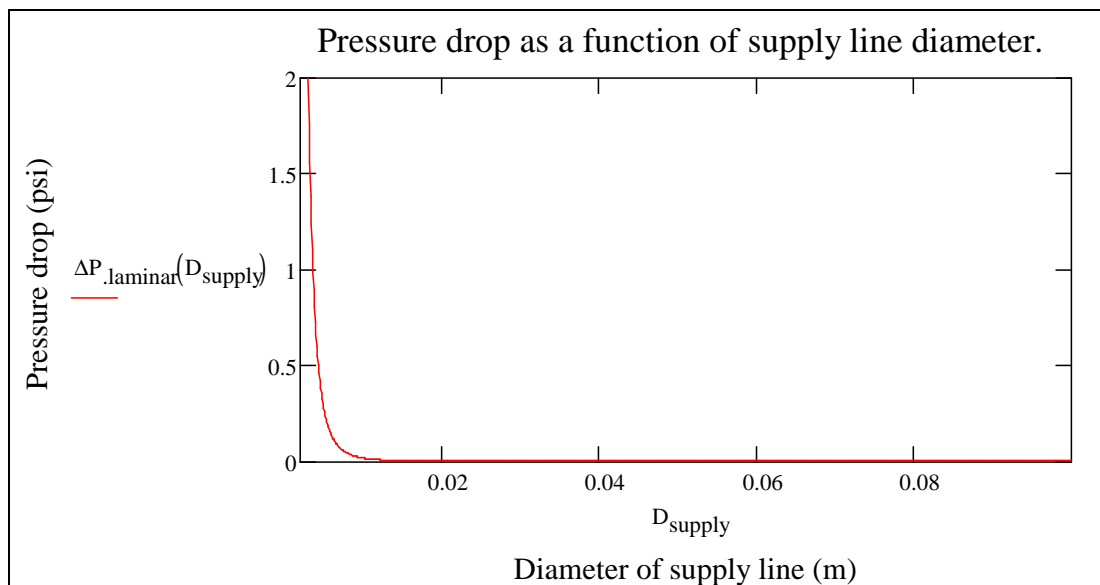
And

$$V_{\text{supply}} = \frac{M_{\text{array}}}{\rho_{\text{air}} \cdot A_{\text{supply}}} \quad A_{\text{supply}} = \frac{\pi}{4} \cdot D_{\text{supply}}^2$$

Combining Equations and simplifying Gives

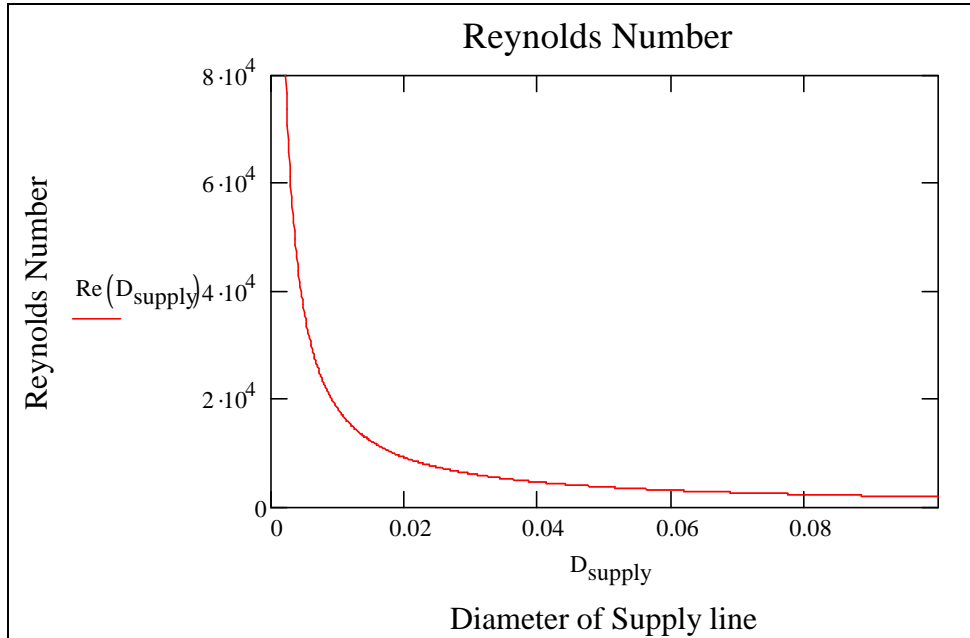
$$\Delta P_{\text{laminar}}(D_{\text{supply}}) := \frac{128 \cdot \mu_{\text{air}}}{M_{\text{array}} \cdot \rho_{\text{air}} \cdot \pi} \cdot L_{\text{supply}} \left(\frac{M_{\text{array}}}{D_{\text{supply}}^2} \right)^2$$

$$\Delta P_{\text{laminar}}(8\text{cm}) = 4.367 \times 10^{-6} \text{ psi}$$



The Graph above is relevant for laminar flow only. For this condition the Reynolds number must be less than 2300. This occurs for diameters greater than 8cm.

$$\text{Re}(D_{\text{supply}}) := \frac{\rho_{\text{air}} \cdot \frac{M_{\text{array}}}{\rho_{\text{air}} \cdot \left(\frac{\pi}{4} \cdot D_{\text{supply}}^2\right)} \cdot D_{\text{supply}}}{\mu_{\text{air}}} \quad \text{Re}(8\text{cm}) = 2.297 \times 10^3$$



The figure above shows the Reynolds number as a function of the diameter of the intermediate supply line. Laminar flow is valid at about 8cm which is impractically large for the current application.

Turbulent flow analysis

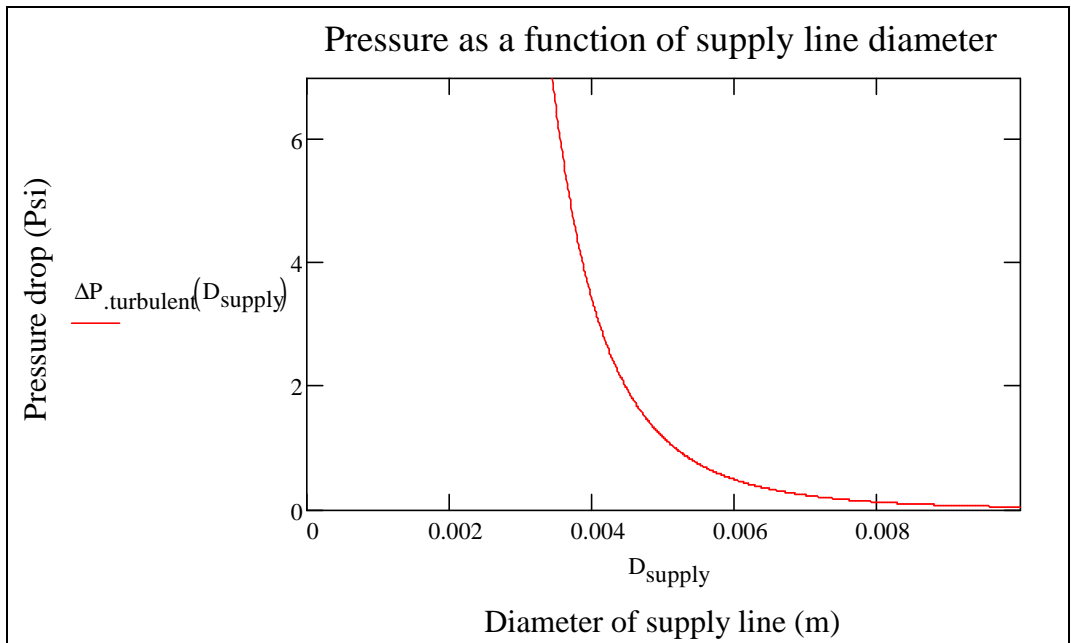
This analysis is valid for Reynolds numbers greater than 4000. This occurs at a diameter of approximately 4.5cm. To maintain incompressible flow analysis the pressure drop should be less than 7.4 psi for this supply line.

Assuming Turbulent flow in the supply line changes the friction factor to the following,

$$f = (0.790 \cdot \ln(\text{Re} - 164))^{-2} \quad \text{From Thermal fluid Sciences second edition, Cengel p. 883}$$

$$\Delta P_{\text{turbulen}}(D_{\text{supply}}) := \left(0.790 \cdot \ln \left(\frac{M_{\text{array}}}{\frac{\pi}{4} \cdot D_{\text{supply}} \cdot \mu_{\text{air}}} - 164 \right) \right)^{-2} \cdot \frac{L_{\text{supply}} \rho_{\text{air}} \left[\frac{M_{\text{array}}}{\rho_{\text{air}} \left(\frac{\pi}{4} \cdot D_{\text{supply}}^2 \right)} \right]^2}{2D_{\text{supply}}} \quad \text{C}$$

$\Delta P_{\text{turbulen}}(6\text{mm}) = 0.489 \text{ psi}$ Pressure drop for intermediate supply line.



The figure above shows the drop in pressure for the intermediate supply line. This graph is valid for diameters less than 4.5 cm. Notice how the pressure drop increases asymptotically for diameter less than 4mm. From this a diameter of 6mm was chosen.

Calculate the Number of the small supply lines.

Number of Supply Lines

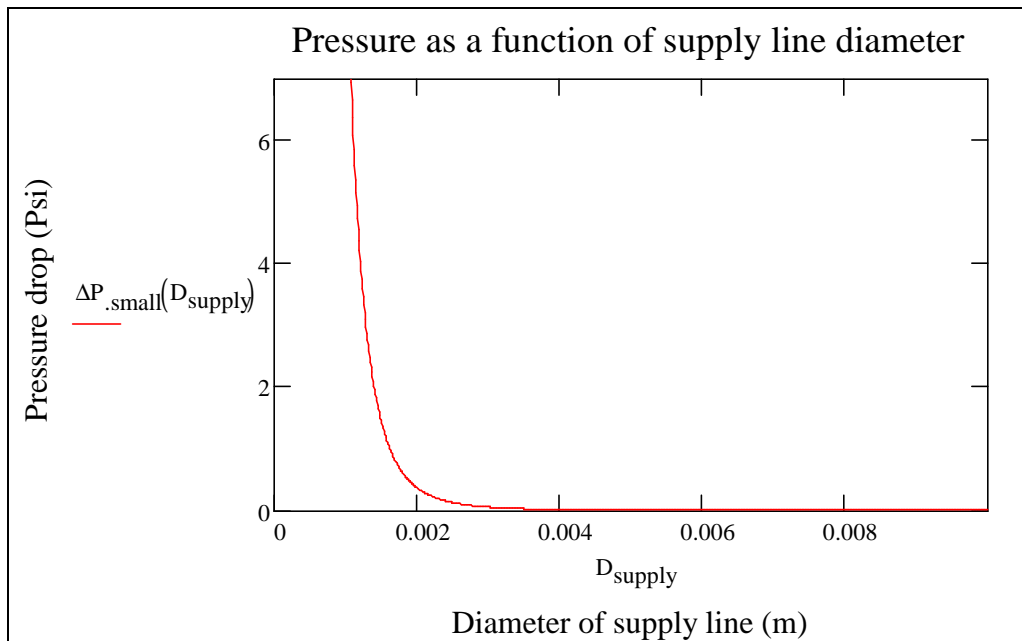
$$N_{\text{small}} \equiv 8$$

Assuming Turbulent flow,

$$\Delta P_{\text{small}}(D_{\text{supply}}) := \left(0.790 \cdot \ln \left(\frac{\frac{M_{\text{array}}}{N_{\text{small}}}}{\frac{\pi}{4} \cdot D_{\text{supply}} \cdot \mu_{\text{air}}} \right) - 164 \right)^{-2} \cdot \frac{L_{\text{small}} \rho_{\text{air}} \left[\frac{\frac{M_{\text{array}}}{N_{\text{small}}}}{\rho_{\text{air}} \left(\frac{\pi}{4} \cdot D_{\text{supply}}^2 \right)} \right]^2}{2 D_{\text{supply}}}$$

$$\Delta P_{\text{small}}(D_{\text{small}}) = 1.102 \text{ psi}$$

Pressure drop across the small supply lines

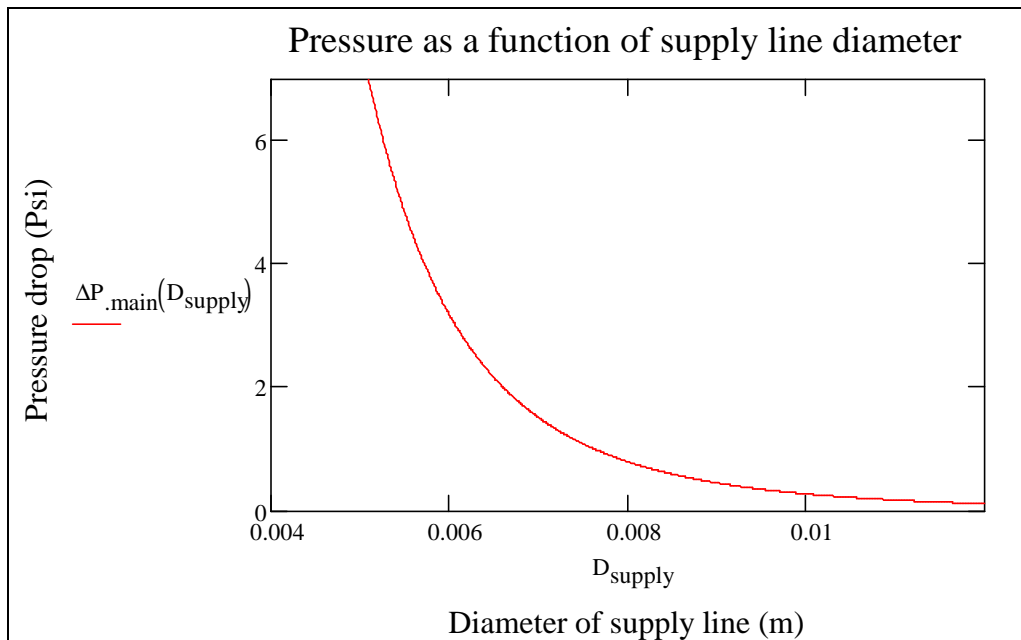


The figure above shows the diameter of the small supply lines is fixed because the microjets are 2.3mm square and a supply lines of 1.6mm is the largest that will physically connect to the microjets. Iteratively increasing the number of supply lines feeding each microjets a value of 8 supply line per microjet array is found.

Losses in the main supply line

$$\Delta P_{\text{main}}(D_{\text{supply}}) := \left(0.790 \cdot \ln \left(\frac{M_{\text{total}}}{\frac{\pi}{4} \cdot D_{\text{supply}} \cdot \mu_{\text{air}}} - 164 \right) \right)^{-2} \cdot \frac{L_{\text{main}} \rho_{\text{air}} \left[\frac{M_{\text{total}}}{\rho_{\text{air}} \left(\frac{\pi}{4} \cdot D_{\text{supply}}^2 \right)} \right]^2}{2 D_{\text{supply}}}$$

$$\Delta P_{\text{main}}(1\text{cm}) = 0.271 \text{ psi}$$



Calculating losses at various fittings, "Minor Losses."

Basic Loss equation

$$\Delta P = K_L \cdot \frac{V^2 \cdot \rho_{\text{air}}}{2}$$

Minor loss coefficient for connection to microjets

$$K_{L_jet} := 1$$

Losses at the connection to microjets

$$\Delta P_{\text{minor_a}} := \frac{K_{L_jet} \left[\frac{\frac{M_{\text{array}}}{N_{\text{small}}}}{\rho_{\text{air}} \cdot \left(\frac{\pi}{4} \cdot D_{\text{small}}^2 \right)} \right]^2 \cdot \rho_{\text{air}}}{2}$$

$$\Delta P_{\text{minor_a}} = 1.004 \text{ psi}$$

Minor loss coefficient for connection to the manifold

$$K_{L_man} := .5$$

$$\Delta P_{\text{minor_b}} := \frac{K_{L_man} \left[\frac{\frac{M_{\text{array}}}{N_{\text{small}}}}{\rho_{\text{air}} \cdot \left(\frac{\pi}{4} \cdot D_{\text{small}}^2 \right)} \right]^2 \cdot \rho_{\text{air}}}{2}$$

Minor loss for the manifold connecting the small lines to the intermediate lines.

$$\Delta P_{\text{minor_b}} = 0.502 \text{ psi}$$

Minor loss for the manifold connecting the intermediate lines to the main line.

$$\Delta P_{\text{minor_c}} := \frac{K_{L_man} \left[\frac{\frac{M_{\text{array}}}{N_{\text{small}}}}{\rho_{\text{air}} \cdot \left[\frac{\pi}{4} \cdot (6\text{mm})^2 \right]} \right]^2 \cdot \rho_{\text{air}}}{2}$$

$$\Delta P_{\text{minor_c}} = 0.163 \text{ psi}$$

Total Pressure Drop For Air Supply System

$$\Delta P_{\text{total}} := \Delta P_{\text{turbulen}}(6\text{mm}) + \Delta P_{\text{small}}(D_{\text{small}}) + \Delta P_{\text{main}}(1\text{cm}) + \Delta P_{\text{minor}_a} + \Delta P_{\text{minor}_b} + \Delta P_{\text{minor}_c}$$

Total Pressure Drop

$$\Delta P_{\text{total}} = 3.532 \text{ psi}$$

Comparing Area Ratios For the small Supply line and the microjets they supply.

Area of microjets per supply line. $A_{\text{jet}} := \frac{\pi}{4} \cdot (.4\text{mm})^2 \cdot 7.62$ $A_{\text{jet}} = 9.576 \times 10^{-7} \text{ m}^2$

Area of Small supply lines $A_{\text{small}} := \frac{\pi}{4} \cdot (1.6\text{mm})^2$ $A_{\text{small}} = 2.011 \times 10^{-6} \text{ m}^2$

Weight Of tubing

Small tubing $W_{\text{small}} := 1.5\text{gm}$

Number of small tubes $N_{\text{small}} := 8 \cdot 6$

Intermediate tubing $W_{\text{intermediate}} := 36\text{gm}$

Number of intermediate tubes $N_{\text{intermediate}} := 6$

Mass of main line $W_{\text{main}} := 13\text{gm}$

Total mass of supply lines

$$W_{\text{total}} := W_{\text{small}} N_{\text{small}} + W_{\text{intermediate}} N_{\text{intermediate}} + W_{\text{main}}$$

$$W_{\text{total}} = 0.531 \text{ lb}$$

Appendix D

This appendix shows the calculations for the location of the wing support bars, or struts. The location along the wing and fuselage must be determined to increase stability and support for the wings.

This file shows the variation of the compression force applied to the wings from the struts when the vertical mounting distance is changed (from the bottom of the fuselage and extended lower)

Distance from the fuselage to the location of the lift force

$$x_L := \frac{\frac{73.5}{2} - 3.875}{2} \text{ in}$$

$$x_L = 16.438 \text{ in}$$

Height of the strut (from the bottom of the wing to the bottom of the mount on the fuselage)

$$h := 6.5 \text{ in}, 6.75 \text{ in}.. 8 \text{ in}$$

Chosen location (along the wing) to place the strut's mount

$$x := 16.438 \text{ in}$$

Fixed at halfway down the wing

Maximum lift force = 2x the weight

$$F_L := 16 \text{ lbf}$$

Equations:

$$\theta(h) := \text{atan}\left(\frac{x}{h}\right)$$

$$M_L := F_L \cdot x_L$$

$$M_L = 21.917 \text{ lbf} \cdot \text{ft}$$

$\theta(h) =$	deg
68.425	
67.675	
66.934	
66.2	
65.475	
64.758	
64.049	

Balance of Moments

$$0 = M_L - T_y \cdot x$$

where T_y is the y-component of the tension force caused by the struts

$$T_y := \frac{M_L}{x}$$

$$T_y = 16 \text{ lbf}$$

The vertical component doesn't change

$$T_x(h) := T_y \cdot \tan(\theta(h))$$

$T_x(h) =$	lbf
40.462	
38.963	
37.571	
36.276	
35.067	
33.935	
32.875	

This file shows the variation of the compression force applied to the wings from the struts when the horizontal mounting distance is changed (from the side of the fuselage and extended further outward)

Distance from the fuselage to the location of the lift force

$$x_L := \frac{\frac{73.5}{2} - 3.875}{2} \text{ in}$$

$x_L = 16.438 \text{ in}$

Height of the strut (from the bottom of the wing to the bottom of the mount on the fuselage)

$h := 6.5 \text{ in}$ Fixed at the bottom of the fuselage

Chosen location (along the wing) to place the strut's mount

$x := 16.438 \text{ in}, 16.688 \text{ in}.. 17.938 \text{ in}$

Maximum lift force = 2x the weight

$F_L := 16 \text{ lbf}$

Equations:

$$\theta(x) := \text{atan}\left(\frac{x}{h}\right)$$

$$M_L := F_L \cdot x_L$$

$M_L = 21.917 \text{ lbf} \cdot \text{ft}$

$\theta(x) =$	
68.425	deg
68.719	
69.006	
69.285	
69.557	
69.823	
70.082	

Balance of Moments

$0 = M_L - T_y \cdot x$ where T_y is the y-component of the tension force caused by the struts

$$T_y(x) := \frac{M_L}{x}$$

$$T_x(x) := T_y(x) \cdot \tan(\theta(x))$$

$T_x(x) =$	
40.462	lbf
40.462	
40.462	
40.462	
40.462	
40.462	
40.462	

$T_y(x) =$	
16	lbf
15.76	
15.527	
15.301	
15.082	
14.869	
14.662	

The compression force does not change

Appendix E

This section shows the reduction in minimum controllable airspeed with the microjets on. Also, the velocity as a function of the weight of the airplane has been graphed. The drag force has also been calculated.

Velocity Calculations

$$C_L := 1.7 \quad \text{form theory of wing sections, Ira page 3}$$

$$M_{\text{plan}} := 8\text{ lbf} \quad \text{weight of plane}$$

$$\rho_{\text{air}} := 1.184 \frac{\text{kg}}{\text{m}^3}$$

$$\text{velocity of plane} \quad V_1 := \sqrt{\frac{M_{\text{plan}}^2}{6 \cdot \text{ft} \cdot 1 \cdot \text{ft} \cdot \rho_{\text{air}} \cdot C_L}}$$

$$V_1 = 17.816 \frac{\text{mile}}{\text{hr}}$$

$$V_1 = 7.965 \frac{\text{m}}{\text{s}}$$

From Flight Control using synthetic jets, Amitay

16 % increase in lift

$$C_{L2} := C_L \cdot 1.16 \quad \text{coefficient of lift}$$

$$V_2 := \sqrt{\frac{M_{\text{plan}}^2}{6 \cdot \text{ft} \cdot 1 \cdot \text{ft} \cdot \rho_{\text{air}} \cdot C_{L2}}}$$

$$V_2 = 24.262 \frac{\text{ft}}{\text{s}}$$

$$\Delta V := V_1 - V_2 \quad \text{Reduction in velocity with the jets activated}$$

$$\Delta V = 1.869 \frac{\text{ft}}{\text{s}} \quad \Delta V = 1.274 \frac{\text{mile}}{\text{hr}}$$

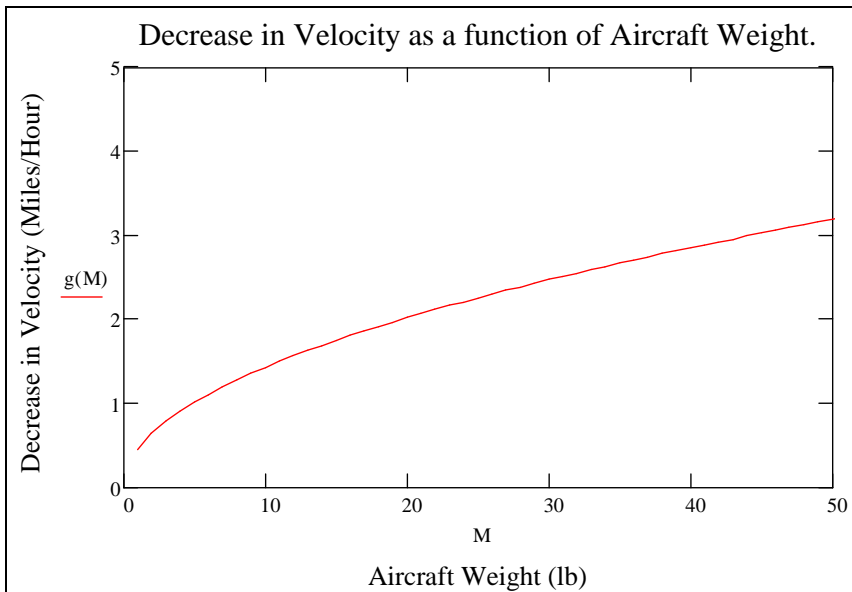
$$\frac{\Delta V}{V_1} = 7.152 \% \quad \text{\% reduction}$$

Change of velocity as a function of weight

$$f(M) := \left(\sqrt{\frac{M \cdot \text{lbf} \cdot 2}{6 \cdot \text{ft} \cdot 1 \cdot \text{ft} \cdot \rho_{\text{air}} \cdot C_L}} - \sqrt{\frac{M \cdot \text{lbf} \cdot 2}{6 \cdot \text{ft} \cdot 1 \cdot \text{ft} \cdot \rho_{\text{air}} \cdot C_{L2}}} \right)$$

M := 1 .. 100

$$g(M) := \left(\sqrt{\frac{M \cdot \text{lbf} \cdot 2}{6 \cdot \text{ft} \cdot 1 \cdot \text{ft} \cdot \rho_{\text{air}} \cdot C_L}} - \sqrt{\frac{M \cdot \text{lbf} \cdot 2}{6 \cdot \text{ft} \cdot 1 \cdot \text{ft} \cdot \rho_{\text{air}} \cdot C_{L2}}} \right) \cdot \frac{1}{5.28 \times 10^3} \cdot 3600$$



$$P(M) := \frac{\sqrt{\frac{M \cdot \text{lbf} \cdot 2}{6 \cdot \text{ft} \cdot 1 \cdot \text{ft} \cdot \rho_{\text{air}} \cdot C_L}} - \sqrt{\frac{M \cdot \text{lbf} \cdot 2}{6 \cdot \text{ft} \cdot 1 \cdot \text{ft} \cdot \rho_{\text{air}} \cdot C_{L2}}}}{\sqrt{\frac{M \cdot \text{lbf} \cdot 2}{6 \cdot \text{ft} \cdot 1 \cdot \text{ft} \cdot \rho_{\text{air}} \cdot C_L}}}$$

Drag Calculations

$$A_{\text{wing}} := 6 \text{ft} \cdot 1 \text{ft}$$

$$C_D := .48$$

Drag at 30 deg. Angle of Attack.

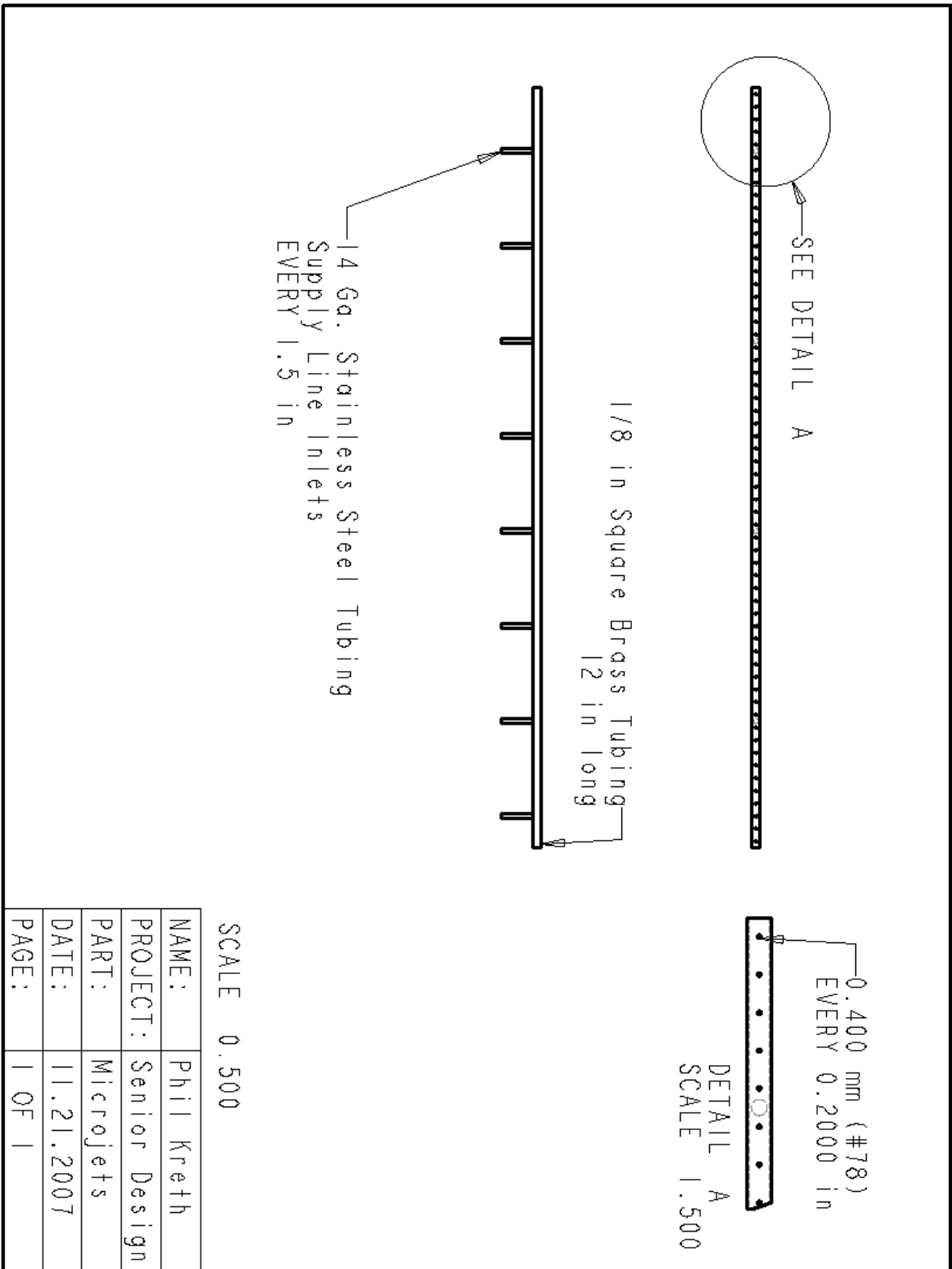
$$F_D := C_D \cdot 5 \rho_{\text{air}} V_1^2 \cdot A_{\text{wing}}$$

$$F_D = 2.259 \text{ lbf}$$

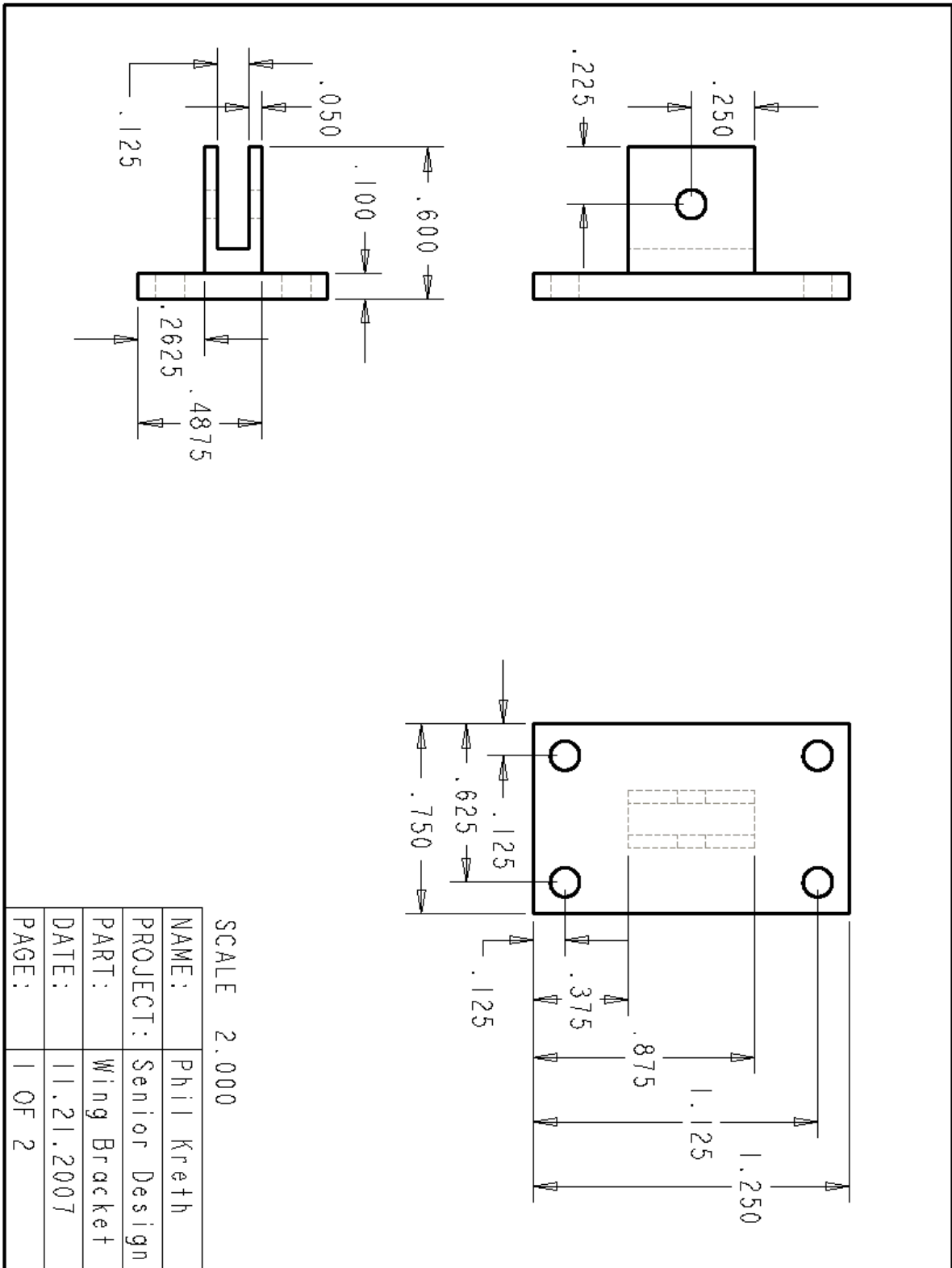
$$F_D = 10.048 \text{ N}$$

Appendix F – All Pro/ENGINEER Drawings and Assembly Views

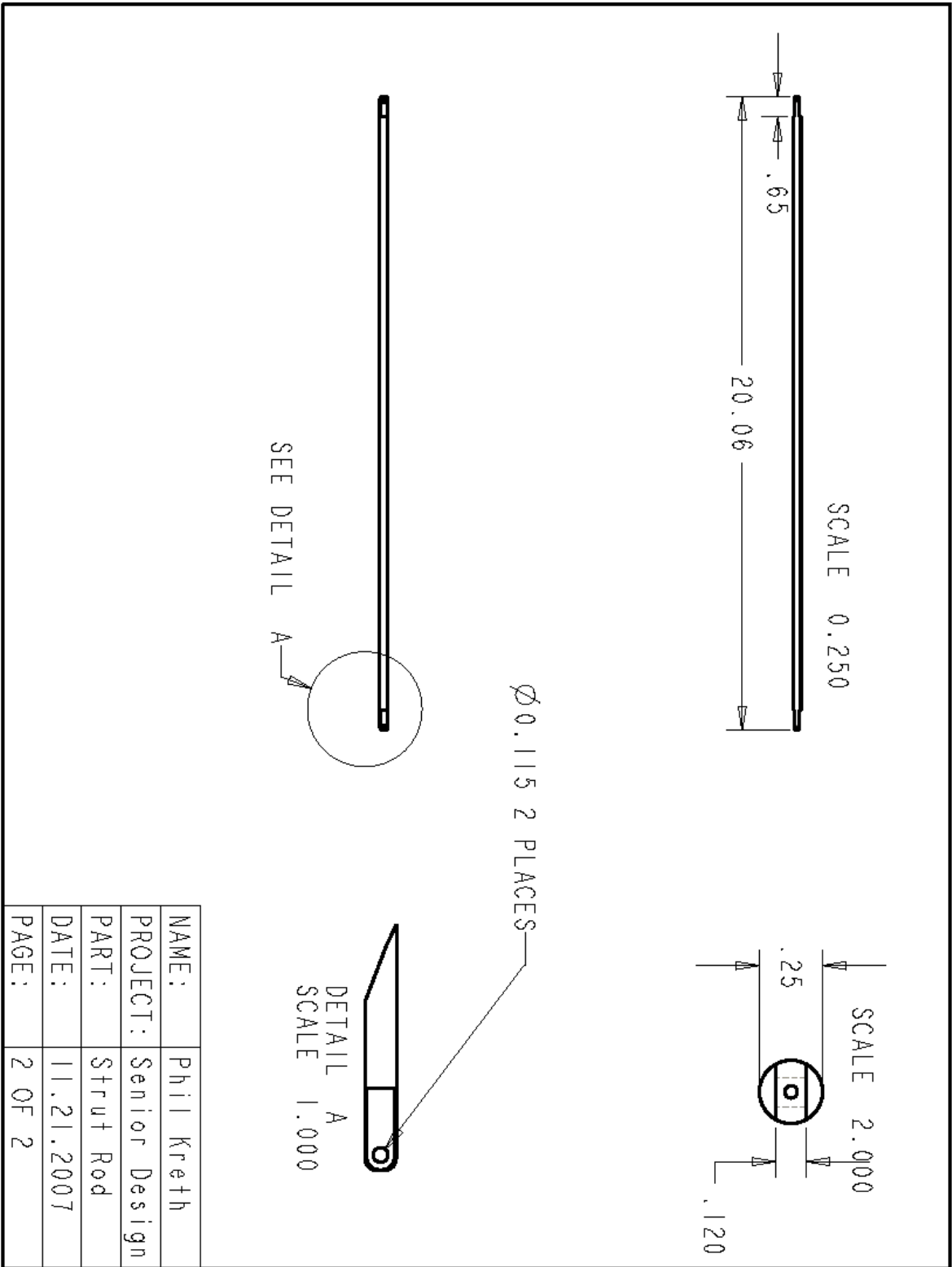
Microjets



Wing Bracket

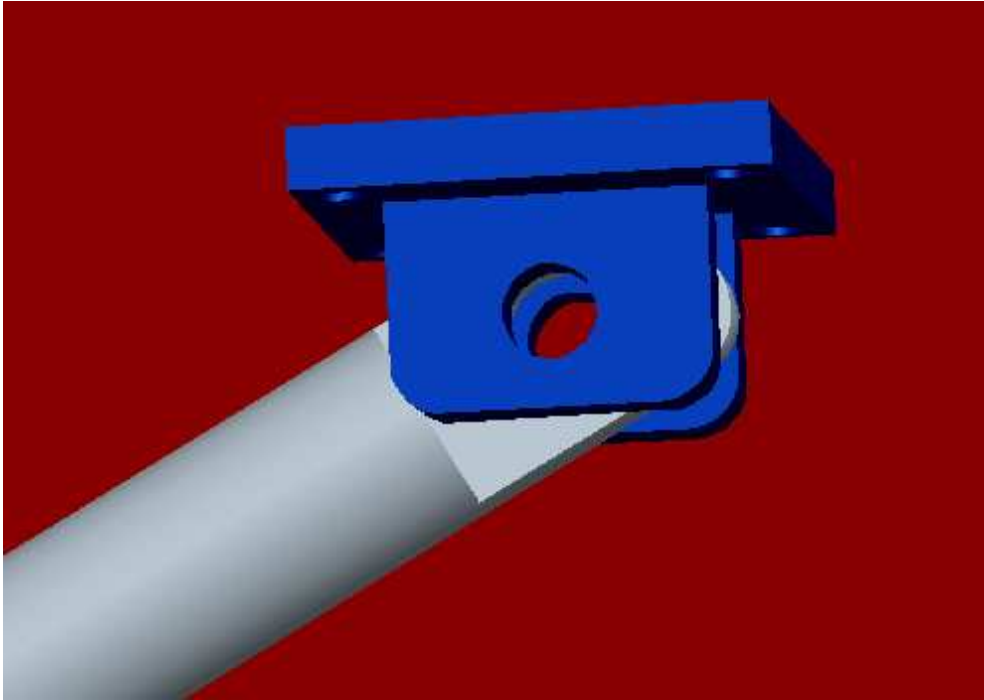


Wing Support Bar

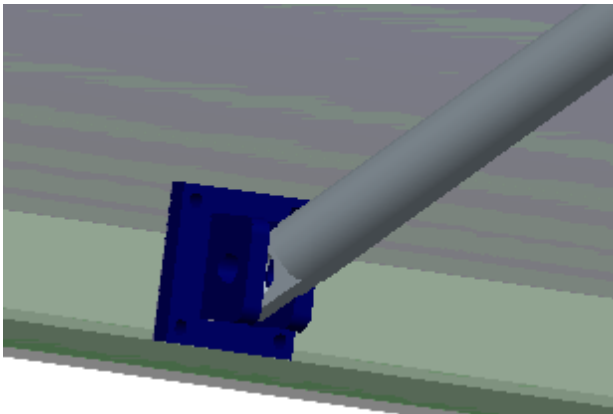


NAME:	Phil Kreth
PROJECT:	Senior Design
PART:	Strut Rod
DATE:	11.21.2007
PAGE:	2 OF 2

Strut System Assembly Views

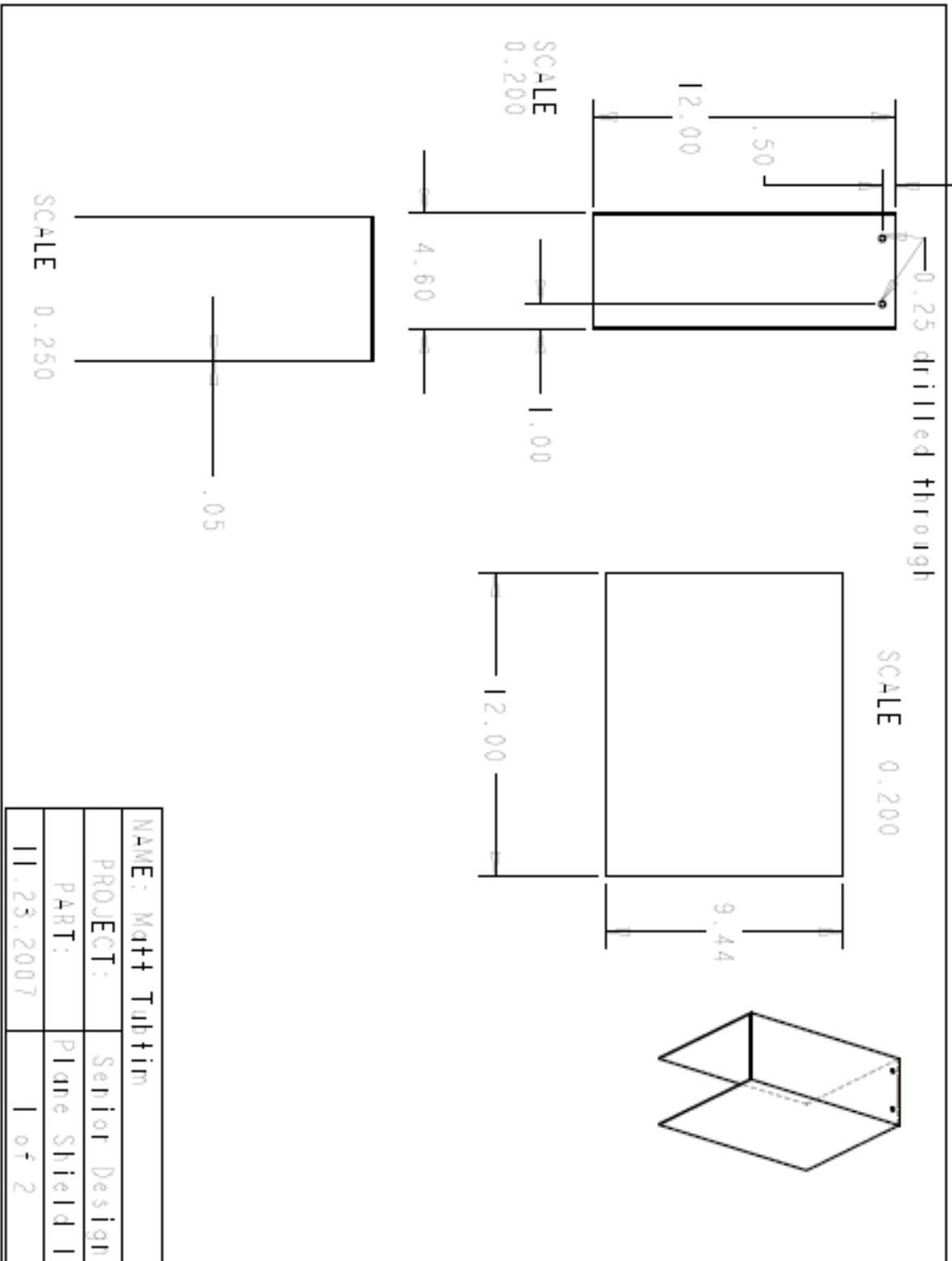


Close-up of the bracket and strut connection. We will accomplish this connection by using a screw and nut for easy removal.

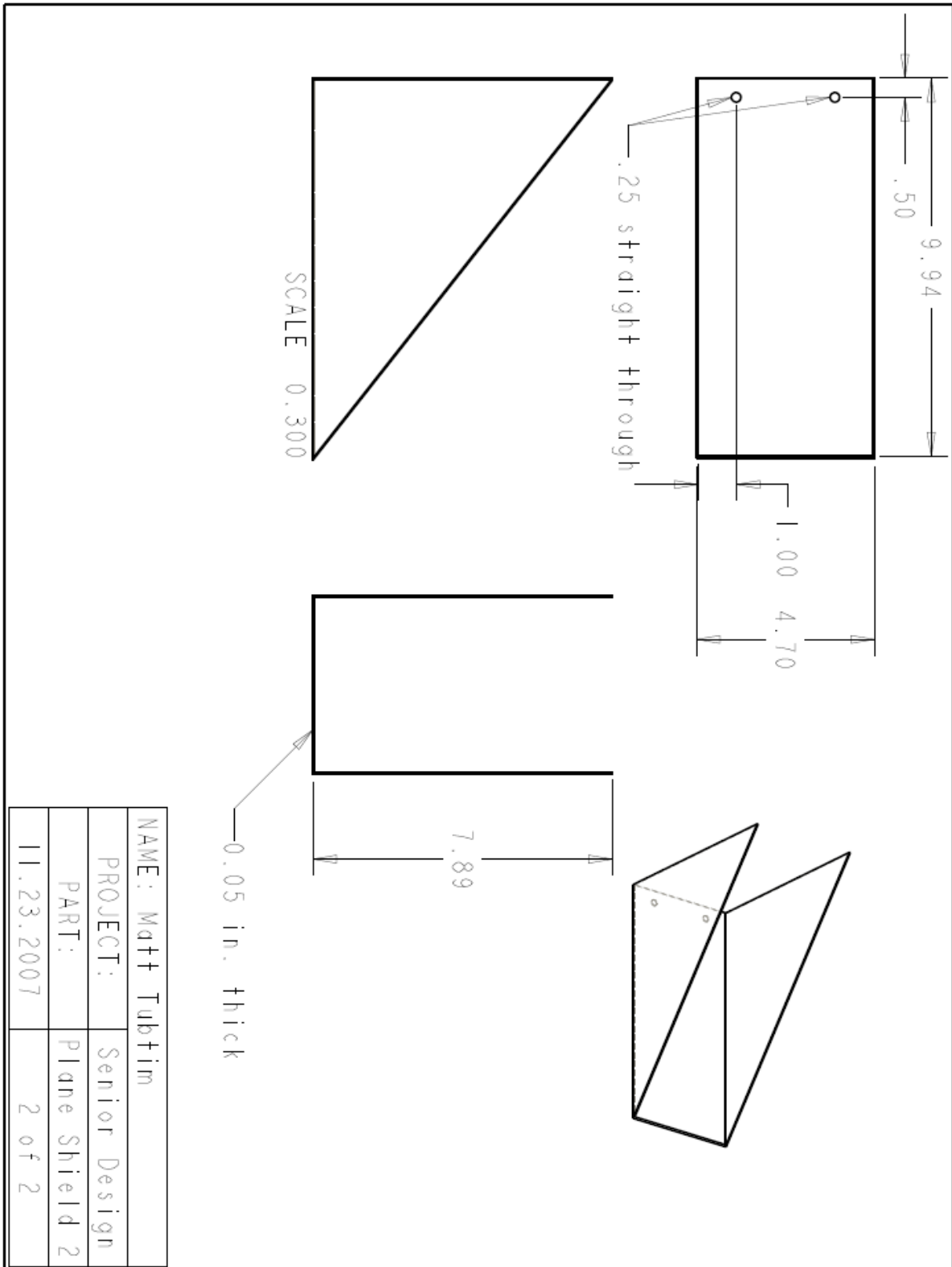


Close-up of the bracket's location at the bottom of the shielding system. The struts will be aligned with the center of gravity of the airframe.

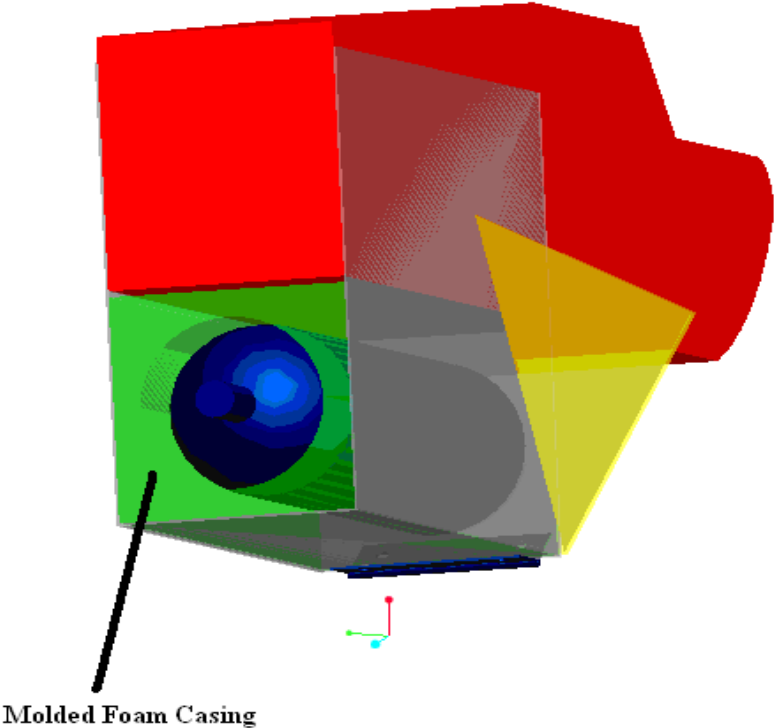
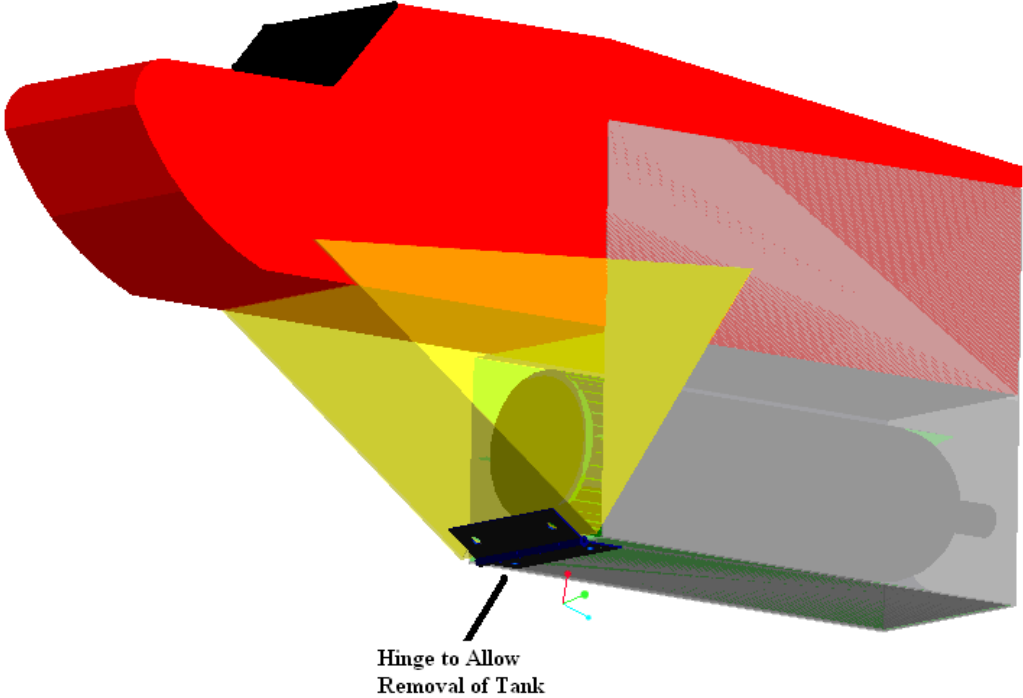
Tank Shielding Part1

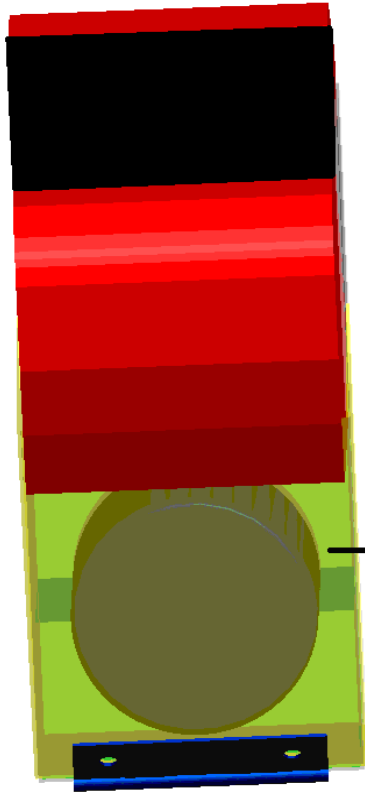


Tank Shielding Part2



Tank Shield Assembly Views





Tank Shown Outside of Plane
To Show Foam Support

Appendix G

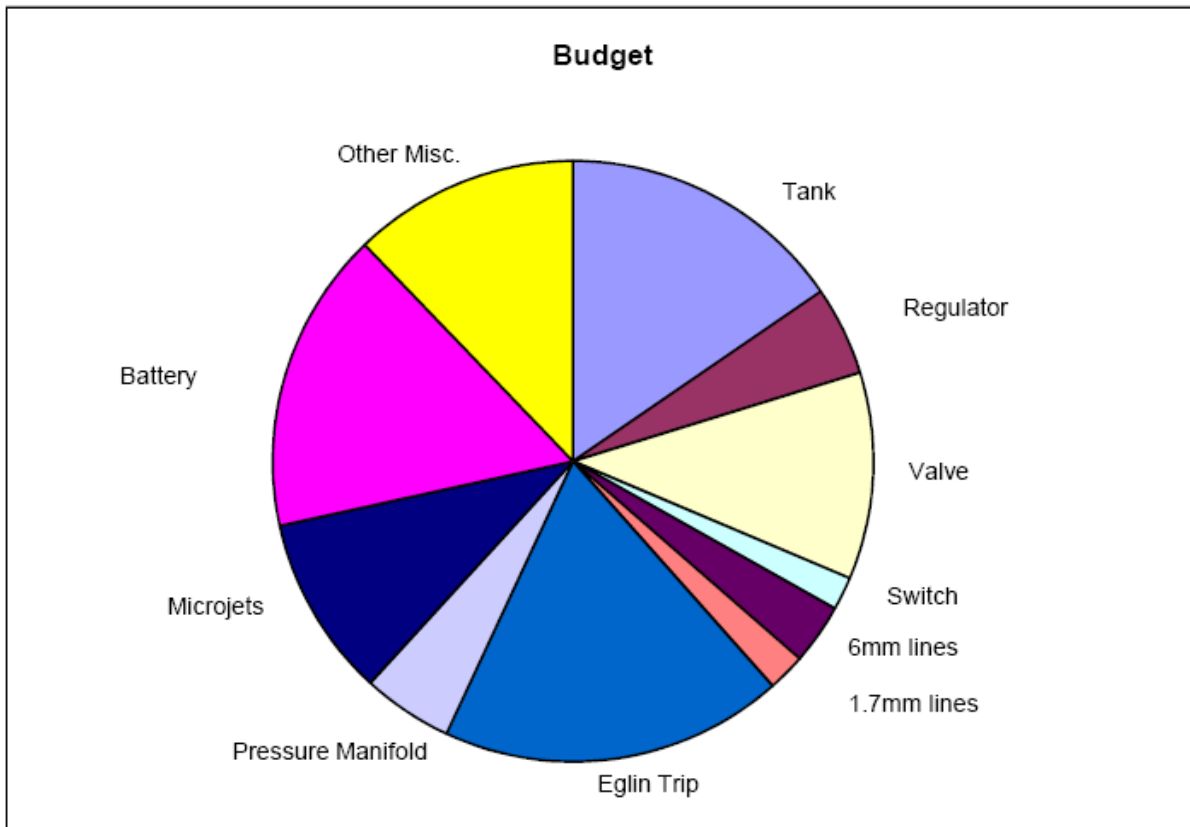
The following table depicts the estimated weight of each item that will be added to the aircraft.

Additional Weight Considerations	
Item	Weight (lbs.)
<i>Tank + Regulator</i>	3.02
<i>Manifold (7x)</i>	0.25
<i>Microjets (6x)</i>	0.25
<i>Lines (56.66 ft)</i>	0.71
<i>Shielding</i>	1.50
<i>Camera</i>	0.02
<i>Struts</i>	0.33
<i>Misc.</i>	+/- 0.50
	Total: 6.08 lbs. (+/- 0.50)

Appendix H

Budget

	Cost	Shipping	20% increase	Taxes	Supplier	Total
Tank	\$189.90	\$0.00	\$227.88	\$17.09	PunisherPB	\$244.97
Regulator	\$59.00	\$0.00	\$70.80	\$5.31	PunisherPB	\$76.11
Solenoid valve	\$137.04	\$0.00	\$164.45	\$12.33	Small Parts	\$176.78
Reciever Switch	\$22.00	\$0.00	\$26.40	\$1.98	Small Parts	\$28.38
6mm lines	\$40.00	\$0.00	\$48.00	\$3.60	Small Parts	\$51.60
1.7mm lines	\$25.00	\$0.00	\$30.00	\$2.25	Small Parts	\$32.25
Eglin Trip	\$293.30	\$0.00	\$293.30	\$0.00	Personal	\$293.30
Pressure Manifold	\$60.00	\$0.00	\$72.00	\$5.40	Small Parts	\$77.40
Microjets	\$120.00	\$0.00	\$144.00	\$10.80	Hobby Town	\$154.80
Battery Packs	\$200.00	\$0.00	\$240.00	\$18.00	Hobby Town	\$258.00
Other misc	\$150.00	\$0.00	\$180.00	\$13.50	Misc.	\$193.50
Overall Total	\$1,296.24	\$0.00	\$1,496.83	\$90.26		\$1,587.09



Appendix I

Planning and Scheduling

The following are definitions of tasks that are listed on the Gantt chart. This schedule was created early in the project. Some aspects have been changed: for example, smoke wire testing was discontinued. The reasons for the change will be discussed in the report in the relevant sections. This original schedule is included to show the methodology for completing the project and also because the deviations from the original schedule are minor. The full Gantt chart is placed in Appendix F.

Research Air Supply Method – Evaluate different possibilities for supplying air to the microjet arrays

Brainstorming (Design Possibilities) – Group meeting to discuss all possible supply systems

Design Evaluations – Put numbers to the design possibilities. This is the evaluation stage of all the possible designs

Measuring Devices Research – Group meeting, brainstorming, and design evaluation for devices to measure plane performance

Design Selection – Group meeting to select the air supply method and measuring device utilizing a design matrix

Detailed Design of Air Supply System – Detailed calculations will be performed so that the final product will meet the product specifications. Engineering drawings will also be created

Detailed Design of Airplane Modifications – Modify the airplane to house the air supply system, the measuring devices, and the additional weight. Weight and balance of the airplane with have to be considered

Purchasing Parts – This represents a deadline that the team needs to meet to order the parts required.

Build Actuators for the Test Model – This is our first iteration of microjets. These will be placed across the entire airfoil used in the wind tunnel testing

Implementing the Actuators – The airfoil for the wind tunnel testing will need to be modified to implement the microjets arrays. For the testing to be relevant the surface conditions of the test section should match that of the airplane wing

Smoke Wire Testing – This is a visualization technique that should show video evidence of separation and also help the team determine where separation occurs and at what angle of attack it occurs. A successful test will show where the flow separates and the location to place the microjets. The following are the requirements for the testing,

- Set up the wind tunnel facility to accept the smoke wire.
- Set up the video recording device.
- Run the wind tunnel from 0 - 10 m/s with the airfoil near the critical angles of attacks. The angles will be manually adjusted during the test to show separated and attached flow. The relevant data will be angle of separation and location

Additional Testing –Smoke wire testing will be performed after the microjets have been implemented to demonstrate flow reattachment. This gives the team additional time in case there are any problems. If necessary this time can be used for different visualization tests. Additional testing may also use a force balance to measure lift and drag improvements on the airfoil.

Evaluating Results – Results will be evaluated from all previous tests and any additional modifications that need to be done will be completed

Machining Microjets – This time will be used to build the microjets that will be implemented on the airplane

Implementing Air System on Airplane – This will be a significant part of the project. The air system must fit on the airplane and have proper weight and balance

Testing – This is the flight testing portion of the project

Evaluate Data / Additional Testing – The data will be evaluated and any additional testing can be performed in the event of bad weather during the first flight testing period

Deliver Product – The product should be ready to deliver to the customer

Appendix J

